ACS NANO

www.acsnano.org

REVIEW

Active Synthetic Microrotors: Design Strategies and Applications

Xianglong Lyu, Jingyuan Chen, Ruitong Zhu, Jiayu Liu, Lingshan Fu, Jeffrey Lawrence Moran,* and Wei Wang*

Cite This: *ACS Nano* 2023, 17, 11969–11993

Read Online

ACCESS | Metrics & More | Article Recommendations

ABSTRACT: Microrotors are microscopic objects that convert energy stored in the environment into spontaneous rotation, in the form of spinning along an axis, rolling on a surface, or orbiting in circles. Because of its distinct dynamics and the vertical flows around it, a microrotor is potentially useful for applications, including drug delivery, minimally invasive surgery, fluid mixing, and sensing. It is also useful as a model system to probe the collective behaviors among rotating micro-objects. In this review article, we comprehensively review the recent experimental progress in designing, synthesizing, and using microrotors. For applications, particular emphasis is placed on microfluidic mixing, biomedicine, and collective behaviors. In the end, we comment on how microrotors can be made more biocompatible and more controllable and rotate in more ways and the challenges therein. A key feature of this review article is to introduce three ways in which to classify a microrotor: the nature of its rotational behavior (spinners, rollers, or orbiters), the cause of its rotation (whether chiral symmetry is broken by shapes, chemical compositions, or the way energy is applied), and its power source (whether powered by chemical reactions, electric or magnetic fields, light, or ultrasound). This review article will help materials scientists and chemists in designing micromachines and microrotors, help engineers in finding appropriate microrotors for a specific application, and help physicists in finding appropriate model systems.

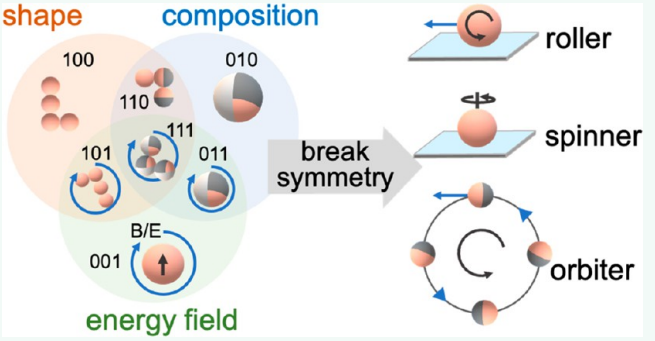

KEYWORDS: *active microrotors, breaking chiral symmetry, spinning, rolling, orbiting, micromotors, catalytic, external fields, biomedical application, collective behavior*

1. INTRODUCTION

Micromachines, which convert ambient energy to motion, have received mounting attention for their ability to move autonomously and to accomplish complicated tasks, such as drug delivery,[1−4] minimally invasive surgery,[5−7] and sensing.[8−10] At the same time, microrotors, which are *rotating* micromachines, have attracted interest for potential applications in microfluidics,[11−14] biomedicine,[15,16] and soft matter physics.[17−20] For example, because they often generate strong vortices, microrotors are very effective for enhanced mixing at low Reynolds numbers. On the other hand, microrotors that interact with each other through hydrodynamics can give rise to various interesting collective behaviors (see section 5 below for details).

Despite the research progress on the fabrication, actuation, and application of microrotors, discussions are limited regarding the guiding strategies for designing and constructing microrotors of controlled geometry and dynamics. In this review, we introduce three complementary schemes to classify microrotors: according to their energy source, according to the mechanism by which ambient energy is converted into the torque that drives rotation, and according to the resulting rotational behavior of the microrotor. Common energy sources include chemical fuels, electric or magnetic fields, or ultrasound. Ambient energy from these sources can be converted into torques by asymmetry in the microrotor's shape, asymmetry in its chemical composition, exposure to a rotational external field, or a combination thereof. These three torque generation mechanisms are then broken

Received: November 22, 2022
Accepted: June 12, 2023
Published: June 20, 2023

https://doi.org/10.1021/acsnano.2c11680
ACS Nano 2023, 17, 11969−11993

Table 1. Comparison among Different Strategies to Design and Fabricate Microrotors, Including Power Sources, Rotation Modes, Fabrication Methods, Mechanism(s) by Which Rotation Is Produced, and Pros and Cons of Each Major Power Source

Power sources	Examples	Modes of rotation[b]	Design strategy[c]	Fabrication methods	Driving mechanisms	Advantages	Limitations
Chemical fuels	Metal microrods[22,23] (section 3.1)	Spinning	010	Electrodeposition or physical vapor deposition	Self-generated chemical gradients (e.g., self-electrophoresis, self-diffusiophoresis)	1. Driving mechanisms well-understood. 2. Various synthesis methods.	1. Poor sample uniformity. 2. Toxic fuels. 3. Bubbles in a population. 4. Particle−particle interactions are complicated for theoretical analysis.
	Tadpole-shaped microrotors[24−28]	Orbiting[a]	110	Chemical synthesis, glancing angle deposition			
	Microgears[29−33]	Spinning	110	Photolithography			
Light	L-shaped microrods[34]	Orbiting[a]	110	Photolithography	Photothermally induced asymmetric fluid flows	Excellent controllability and tunability	Typically require high-energy lasers and complicated experimental setups
	Microdisks[35]	Spinning	001	Photolithography	Transfer of angular momentum of photons		
Magnetic fields	Ni microspheres[36,37]	Spinning or rolling	001	Commercially available	Coupling between rotating magnetic fields and the magnetic dipoles in Ni.	1. Mechanism well-understood. 2. Excellent controllability and tunability. 3. Often exhibit interesting collective behaviors.	1. Typically require a relatively complicated experimental setup. 2. Difficult to actuate or control individual particles.
Electric fields	Patchy particles[38]	Orbiting[a]	110	Dewetting of colloids out of an oil shell	Induced charge electrophoresis (ICEP, see main text for details)		
	Metallic nanorods[39,40]	Spinning	001	Electrodeposition into nanoporous templates, followed by template dissolution	Coupling between a rotating electric field and the electric dipoles in nanowires		
Ultrasound	Metallic nanorods[41−43]	Spinning or orbiting[a]	100	Electrodeposition into nanoporous templates, followed by template dissolution	Acoustic microstreaming and/or nonreciprocal oscillation	1. Powerful. 2. Modes of rotation can be switched by varying ultrasound parameters.	1. Require a relatively complicated experimental setup. 2. Poor sample uniformity. 3. Weak control.

[a]As noted in the main text, all instances of "Orbiting" in this table result from a superposition of spinning (particle rotation about its own axis) and translational motion. For brevity, we refer to this behavior as "Orbiting", but throughout this work, the classification "Orbiting" should be interpreted as "Spinning + Translating". In other words, all Orbiters that we are aware of are also Spinners that happen to translate. We are not aware of any examples of orbiters that spin through an angle greater or less than 2π during one orbit, nor are we aware of any examples of rotors that orbit without spinning at all. Ultrasound-powered metallic nanorod rotors can display either pure spinning motion or orbiting. Under one condition, the rods spin about their long axis. Under a different experimental condition, they orbit in the $x-y$ plane. These two dynamics occur at different conditions and are not related. See section 4.4.1 and 4.4.2 and refs 41−43 for details. [b]See Figure 1 for illustrations. [c]See Figure 2 and section 2 for details.

https://doi.org/10.1021/acsnano.2c11680
ACS Nano 2023, 17, 11969−11993

Table 2. Literature Examples of Microrotors That Use One of the Four Most Common Design Strategies (001, 010, 100, 110)[a]

		Microrotors powered by external fields			
Design strategies	Chemical reactions	Light	Electric fields	Magnetic fields	Ultrasound
001	No report	60−64	39, 40, 65, 66	44, 67−70	41
010	22, 23, 45, 51−53, 71−74	No report	75, 76	No report	No report
100	30−33, 77	78	79	No report	42, 43, 46, 80−82
110	31−33,67,83−87	34, 88	38, 79, 89−91	No report	No report

[a]Individual studies are indicated as reference numbers.

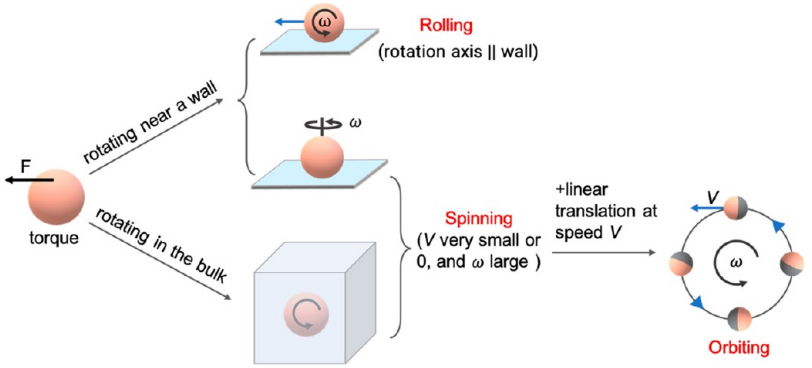

Figure 1. "Decision tree" to determine the rotation modes (rolling, spinning, or orbiting) of a microrotor.

down into seven design strategies, depending on exactly how torques are introduced, using a numbering convention consisting of three digits that can take the value "0" or "1" (e.g., "011"). Once chiral symmetry is broken, a microrotor becomes a spinner, roller, and/or orbiter with distinct dynamics, depending on whether it rotates in the bulk or near an interface and whether the rotational motion is coupled to a translational motion. These three modes of rotation and the seven design strategies are discussed extensively in section 2.

Literature examples are then introduced over the next two sections on microrotors powered by chemical reactions (section 3) or external fields (section 4) such as light, magnetic fields, electric fields, or ultrasound. In each example, we describe the way the rotor moves and assign a proper index that explains its cause of rotation. In section 5, we review microrotors used for microfluidic mixing and biomedicine and their interesting collective behaviors for fundamental research. Finally, we comment in section 6 on a few key issues for the next phase of microrotor development. Two tables (section 2) are given to aid readers: Table 1 compares microrotors powered by various mechanisms including their design strategies, fabrication methods, rotation modes, advantages, and shortcomings. Table 2 lists microrotors designed in various strategies. This comprehensive review is intended to enhance the understanding of how to design a microrotor, how to experimentally realize a design strategy, and what a microrotor can do both in applied settings and for fundamental sciences. We note that a review article (ref 21) was recently published that focuses more on the soft matter physics aspect of microrotors, while this article complements by focusing more on their fabrication, design strategies, experimental realization, and applications.

2. MICROROTORS: ROTATION MODES AND DESIGN STRATEGIES

2.1. Spinning, Rolling, and Orbiting. Translation and rotation are two fundamental modes of motion for micromachines. The distinguishing feature for a microrotor is its ability to roll, spin, or orbit, collectively known as rotation. In this work, we use the word "spin" to refer to a particle rotating about its own axis and "orbit" to refer to translating in a circular trajectory. These two behaviors could coexist in the same particle, in the same sense that the earth's moon spins about its own axis and orbits the earth at the same time.

As illustrated in Figure 1, a microrotor is said to be "rolling" when rotating about an axis parallel to a nearby substrate (along which it translates) and "spinning" when rotating about an axis perpendicular to the substrate and/or spinning about its own axis in the bulk fluid far from a surface. In the "spinning" case, the rotor's center of mass remains stationary; in the "rolling" case, the rotor's center of mass moves along the nearby wall. In the case of an orbiting microrotor, the center of mass moves in a circular trajectory while spinning on its own. Such orbiting motion can be decoupled into translation (at a linear speed of V) and spinning (at an angular speed of ω) so that both its orientation and center of mass location change with time. Simple math reveals that in an ideal case the radius of this microrotor's orbit r is just V/ω. In all instances of orbiters that we review below, the orbiting motion results from a superposition of linear translation and spinning, so that it always spins through an angle 2π during one orbit, as does the earth's moon, a phenomenon called synchronous rotation. (However, the physical origins of synchronous rotation are different in each case: for orbiting microrotors, synchronous rotation derives from the superposition of translation and rotation, while in the case of the Moon it derives from tidal locking.)

2.2. Seven Ways to Break Chiral Symmetry. Breaking chiral symmetry is the key in generating torques for a microrotor, and it is typically achieved in three ways: in the particle shape, in its composition and functionalization, or in the way an energy field is applied (e.g., electric or magnetic fields). As a result, there are in principle $2^3 - 1 = 7$ different strategies to design a microrotor, depending on which of these 3 aspects cause rotation.

https://doi.org/10.1021/acsnano.2c11680
ACS Nano 2023, 17, 11969−11993

A three-digit index consisting of 0 and 1s is assigned to each strategy based on whether rotation is *caused* (1) or not (0) by particle shape, material composition, and an external field (in that order). A "1" is to be inserted in a given spot if that factor is determined to be a proximate cause of the driving torque on the rotor (here "proximate" means immediate or direct, specifically in reference to a causal relationship). These strategies are illustrated in Figure 2.

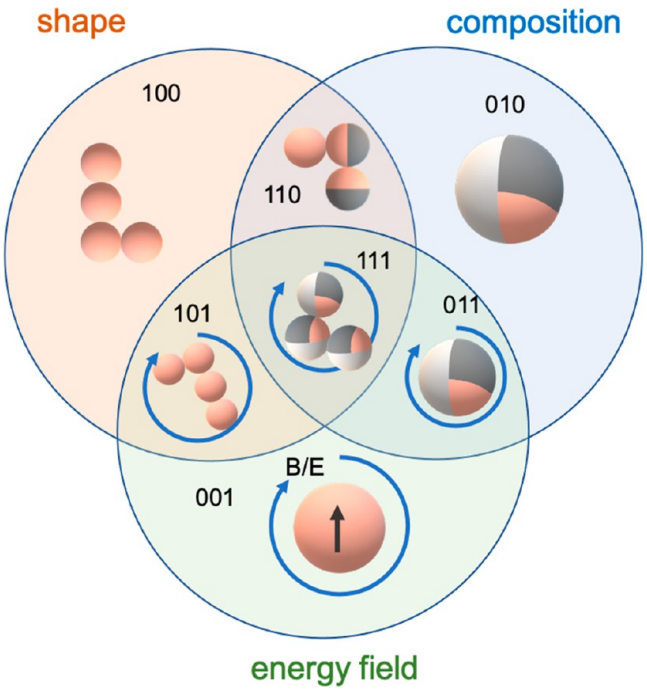

Figure 2. Design strategies of microrotors. A microparticle starts rotating if its chiral symmetry is broken in shape, composition, or the way energy is supplied. The three-digit index corresponds to which aspect is involved in generating rotation of a particular microrotor ("1") or not ("0"). Here, "B" and "E" refer to a magnetic and electric field, respectively, and rotation is illustrated with blue arrows. The black arrow in (001) represents the induced or permanent electrical or magnetic dipole. Different colors on a sphere represent different material compositions or surface chemistry.

(i) Type "001", corresponding to microrotors of achiral shapes (0) and uniform composition (0), subject to a rotational external field that causes particle rotation (1). Typical examples include magnetic microspheres rolling on a substrate in a rotating magnetic field (section 4.2)[44] and metallic nanowires spinning in rotating electric fields (section 4.3).[39]

(ii) Type "010", corresponding to microrotors of an achiral shape (0) yet asymmetric surface functionalization/material composition (1), placed in a uniform energy field (0). A typical example is a microsphere with chirally positioned, chemically active patches, suspended in uniform solutions of fuel molecules (section 3.1).[45]

(iii) Type "100", corresponding to microrotors of chiral shapes (1) but uniform surface properties (0), in a uniformly applied energy field (0). One example is deformed, crooked copper microrods rotating in fuel solutions (section 3.2.1).[22] Other examples include Pt microgears spinning in H_2O_2[30] and metal microgears spinning in uniform ultrasound.[46]

(iv) Type "110", corresponding to microrotors of chiral shapes and asymmetric compositions, in a uniform energy field. One scenario is an asymmetric aggregate (a chiral multimers) made of Janus microspheres in fuel solutions. The propulsive force from each motor then acts together on the center of the mass of the aggregate, generating a torque that rotates it. Examples are given in section 3.3. Other examples include microgears spinning in a bath of active particles,[31−33] L-shaped microparticles rotating under uniform lighting,[34] and tadpole-shaped Janus particles rotating in chemical fuels.[24]

(v) Type "101", corresponding to microrotors of chiral shapes but uniform composition, placed in a nonuniform energy field. Although shape asymmetry alone is often sufficient in inducing rotation, further breaking the uniform of the energy field presents additional possibilities of spatially varying torques. Example includes a metavehicle with chiral metasurface in polarized light.[47]

(vi) Type "011", corresponding to achiral microrotors with chiral compositions, in a nonuniform field. Example includes a microdrone asymmetrically embedded with Au nanorod in its transparent body in polarized light.[48]

(vii) Type "111", corresponding to microrotors with the highest level of design complexity. Any microrotor of the above 6 types can be made into this type by introducing additional torques in the remaining aspect(s), in doing so often providing improved of controllability and tunability for rotation. Examples include a snowman-shaped and Janus microspheres spiraling toward spots of low light intensity[49,50] (section 3.3).

With these strategies, many types of micromotors that move linearly can be transformed into rolling, spinning, or orbiting microrotors. For example, a bimetallic micromotor that moves linearly in H_2O_2 solutions can be transformed into a microrotor by laying the rod on its side and sequentially depositing two different metals on the upward sides, producing a 010 rotor that undergoes orbiting (i.e., translation combined with spinning) (see Figure 3c).[23] As another example, by attaching translational Janus micromotors at specific points on a microgear, the propulsive forces generated by the motors become torques, leading to rotation; this complex constitutes a 110 spinner.[31] A third example consists of translational micromotors organized into clusters that orbit or spin; these rotors are either 010 or 110 depending on their chemical patterning (see Figure 7).[49−53] Finally, Janus micromotors can become orbiting microrotors if the metallic hemisphere is not axially symmetric (110).[24] While we do not claim that *any* type of micromotor can be transformed into *any* type of microrotor, it is possible in principle to modify micromotors in many different ways and in doing so produce microrotors with greater complexity and collective dynamics.

Sections 3 and 4 introduce literature examples of microrotors following these strategies powered by chemical reactions or external fields, respectively. In particular, the first four strategies ("001", "010", "100", and "110") will be described in more details given their simplicity and popularity in the literature. The three-digit index is provided in parentheses for each example when they are first mentioned in the text.

Before we conclude this section on design principles, two special cases of rotation are worth mentioning. First, as in the case of the earth orbiting the sun, a microrotor could also move

https://doi.org/10.1021/acsnano.2c11680
ACS Nano 2023, 17, 11969−11993

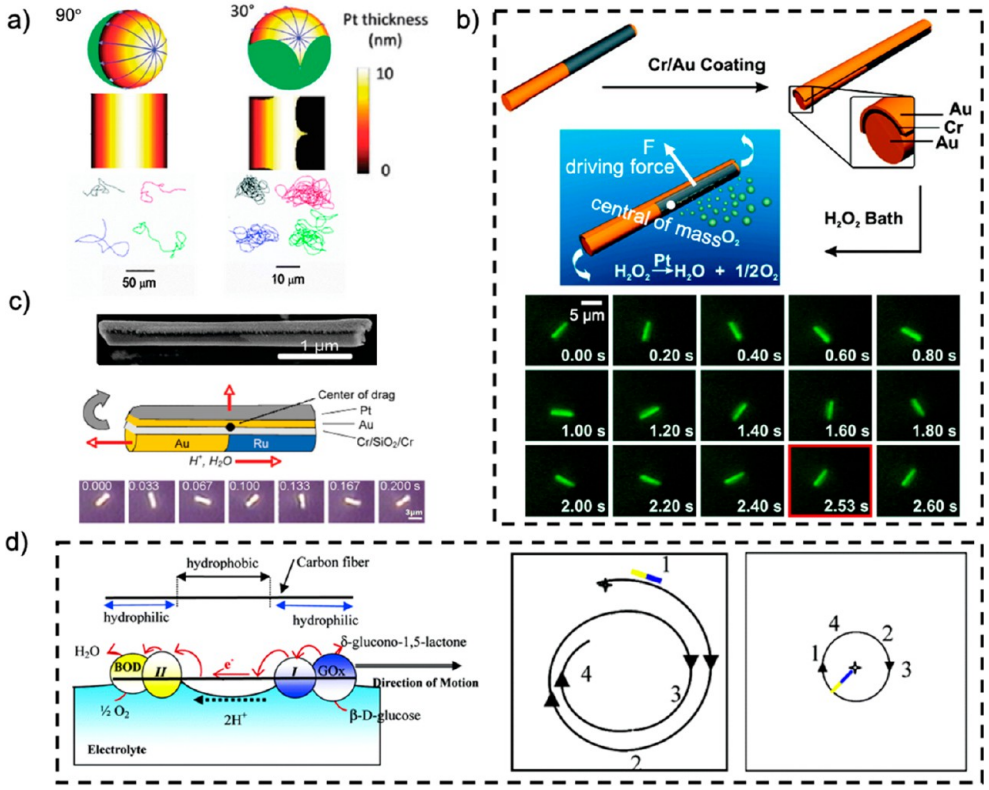

Figure 3. Microrotors of axisymmetric composition ("010"). (a) 3D model (top), 2D layout (middle), and trajectories (bottom) of sphere microrotors with different Pt caps deposited at glancing angles of 90° and 30°. Reprinted with permission under a Creative Commons (CC) BY 3.0 from ref 45. Copyright 2015 Royal Society of Chemistry. (b) Schematic (top) and snapshots (bottom) of a rotating Au−Pt−Au three-segment microrod with Cr/Au deposited on one side of its body. Reprinted with permission from ref 22. Copyright 2007 American Chemical Society. (c) SEM (top), schematic (middle), and snapshots (bottom) of a rotating Au−Ru microrod with Cr/SiO_2/Cr, Au, and Pt layers sequentially deposited on one side of its body. Reprinted with permission from ref 23. Copyright 2009 American Chemical Society. (d) The driving mechanism (left) of a carbon fiber with GOx and BOD on its ends and its trajectories when GOx/BOD > 1 (middle) and GOx/BOD ≫ 1 (right). Reprinted with permission from ref 72. Copyright 2005 American Chemical Society.

in precession so that its rotation axis is neither parallel nor perpendicular to the substrate but rather sweeps through space. This special case of rotation could lead to interesting individual or collective dynamics.[37,54,55] A second case is magnetic helices that spin their bodies in a rotating magnetic field and move linearly.[56,57] Although they are technically "microrotors" because they convert ambient energy to rotation along their long axes, most studies of these microhelices employ rotational motion as a means to bring about translational motion. Since our focus is on microrotors for which rotation is the end goal, we do not emphasize them in this review, even though interesting collective dynamics could arise from interactions (e.g., hydrodynamic or electrostatic interactions) among these rotors.[58,59]

3. CHEMICALLY POWERED MICROROTORS

Chemically powered microrotors can rotate autonomously and independently via catalytic decomposition of chemical fuel, such as H_2O_2, and they move by either self-electrophoresis[92] or self-diffusiophoresis.[93] In these cases, design strategies of "010", "100", and "110" are most common because chemical fuels are typically supplied uniformly throughout the solution.[94]

3.1. Achiral, Catalytic Microrotors ("010"). Micromotors with well-defined, achiral shapes, such as spheres and rods, have received great interest among physicists and materials chemists because of their monodispersity, uniformity, simplicity of production, and potential applications in the fields of biomedical treatment and environmental remediation. At a steady state, the driving force and drag force they receive are equal in magnitude but opposite in direction. As a result, they will move linearly, only disrupted by Brownian motion. If we confine the catalytic reaction to occur only in specific regions of the micromotor, symmetry can be broken for the driving force, and the resulting torque transforms the micromotor into a 010 microrotor.

Archer et al.[45] turned the typical polystyrene-platinum (PS-Pt) Janus spheres that move linearly in H_2O_2 into spherical microrotors through a glancing angle deposition (GLAD) technique ("010"), in which the sample stage is tilted so that the shadowing effect of neighboring particles enables the deposition of asymmetric structures. By changing the glancing angle θ, they limited the Pt cap originally distributed on half of the PS sphere to only coat part of the PS hemisphere, breaking the axial symmetry of the thickness of the Pt cap (Figure 3a). As a result, the electrophoretic propulsion force arising from the uneven distribution of Pt cap thickness became unbalanced, leading to the rotation of these PS-Pt spheres. When $\theta = 20°$, the maximum angular speed reaches a maximum value of ∼16 rad/s in 10% H_2O_2. Similarly, along the same lines, Marine et al. synthesized a spherical bimetallic microrotor by sequentially depositing on an inert microsphere two metals that formed an electrocatalytic pair ("010"). The sphere rotated because of an uneven distribution of mass, which resulted in an uneven fluid drag. This uneven nature of the drag results in "circle swimming", which we refer to in this review as "orbiting" (see Figure 1c).[71]

https://doi.org/10.1021/acsnano.2c11680
ACS Nano 2023, 17, 11969−11993

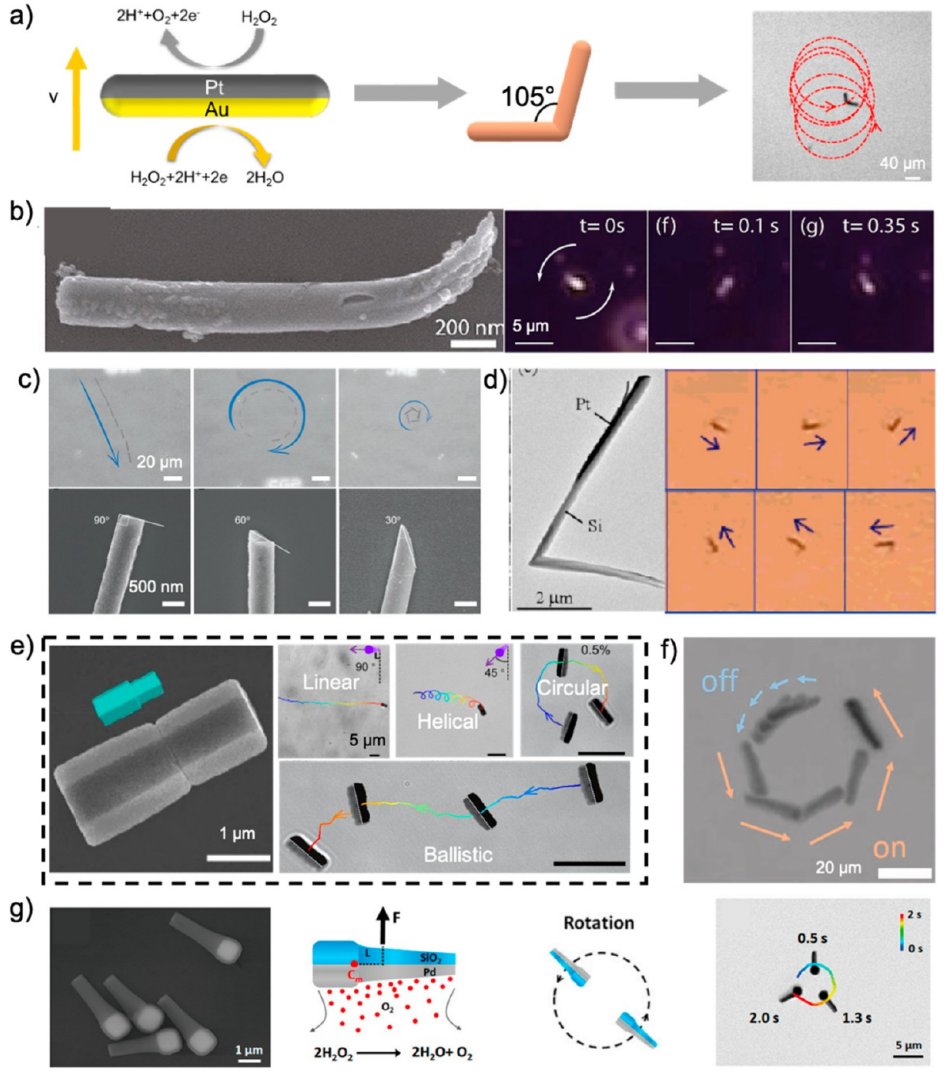

Figure 4. Asymmetric microrod rotors ("100" and "110"). (a) Schematic of the transformation of a Au−Pt bimetallic micromotor into an L-shaped microrotor. Reproduced with permission from ref 83. Copyright 2018 IOP Publishing. (b) SEM image (left) and snapshots (right) of a rotating brush-shaped Cu microrod in Br_2. Reproduced with permission from ref 77. Copyright 2011 American Chemical Society. (c) Overlaid optical micrographs of p−n junction Si nanowires exhibiting different trajectories (top) and the corresponding SEM images (bottom). Reprinted with permission from ref 84. Copyright 2017 Wiley-VCH. (d) SEM images of L-shaped Si−Pt microrods fabricated by GLAD (left) and a sequence of optical micrographs of their rotation (right). Reprinted with permission from ref 85. Copyright 2007 American Chemical Society. (e) SEM image of an asymmetric ZnO microrod (left) and its four modes of motion (right). Reprinted with permission from ref 67. Copyright 2020 American Chemical Society. (f) Overlaid optical micrographs of the orbiting motion of a core−shell $Zn_XCd_{1-X}Se$−Cu_2Se nanowire. Reprinted with permission from ref 86. Copyright 2019 Wiley-VCH. (g) SEM (left), schematic (middle), and overlaid optical micrographs (right) of a matchstick-shaped Fe_2O_3@SiO_2−Pd microrod rotating in H_2O_2. Reprinted with permission from ref 87. Copyright 2021 Royal Society of Chemistry.

Qin et al.[22] turned the classic gold−platinum (Au−Pt) bimetallic rods into spinners by limiting the catalytic decomposition of H_2O_2 on only one end of the rods ("010"). As shown in Figure 3b, they synthesized Au−Pt−Au three-segment rods of 5 μm in length and 360 nm in diameter by electrodeposition with a very short (20 nm in length) Au section on the tip of the Pt end. A bilayer of 10 nm of chromium (Cr)/40 nm of Au was then coated on one side of the three-segment rod. Because of this bilayer, the symmetry of the propulsive force of the metallic rod was broken, rotating the rod at a maximum angular speed of 2.48 rad/s in 3% H_2O_2.

A rod-shaped micromotor starts to move in circular orbits if an additional force is introduced in a direction perpendicular to its direction of translation. As an example, Wang et al.[23] sequentially deposited Cr, SiO_2, Cr, Au, and Pt layers on one side of a Au−Ru bimetallic rod, adding a radial driving force by the self-electrophoresis of the Au−Pt pair and hence rotating the metallic rods (Figure 3c) ("010"). In an aqueous solution containing 15% H_2O_2, these microrods rotate at an average angular speed of ~19 rad/s, and the fastest speed achieved was ~42 rad/s. Mano et al.[72] reported microrotors made of carbon fiber loaded with glucose oxidase (GOx) and bilirubin oxidase (BOD) on opposite tips ("010"). At the air−water interface with low viscous drag, the oxidation of glucose and the reduction of O_2 happened on the GOx and BOD ends of the fiber, respectively, generating a gradient of proton concentration and an electric field parallel to the axis of the fiber. The electric field exerted an electrophoretic force on the charged fiber, causing it to move linearly toward the GOx end (Figure 3d left). This motor moved in circles (Figure 3d right) at ~31.4 rad/s,

https://doi.org/10.1021/acsnano.2c11680
ACS Nano 2023, 17, 11969−11993

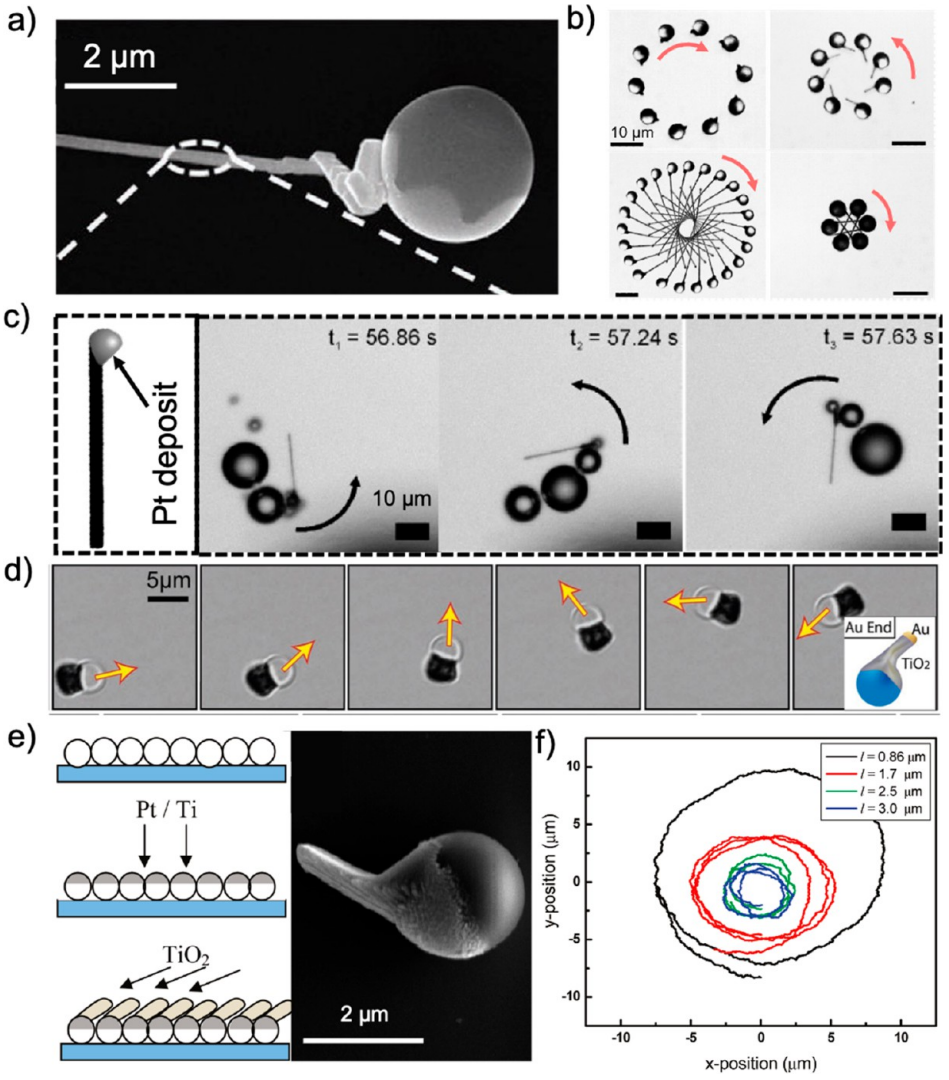

Figure 5. Tadpole-shaped microrotors ("110"). (a) SEM image of a tadpole-shaped microrotor consisting of a PS-Pt Janus microsphere and a Ag tail growing out of the sphere. Reprinted with permission from ref 24. Copyright 2020 Wiley-VCH. (b) Overlaid optical micrographs of a tadpole-shaped microrotor in (a) of different tail lengths rotating in H_2O_2. Reprinted with permission from ref 24. Copyright 2020 Wiley-VCH. (c) Schematic (left) and snapshots (right) of the rotation of a carbon nanotube modified by Pt particles at one end. Reprinted with permission from ref 25. Copyright 2011 Elsevier. (d) Snapshots of the rotation of a SiO_2−TiO_2−Au microrotor. Inset: schematic of the microrotor. Reprinted with permission from ref 26. Copyright 2019 Wiley-VCH. (e) Preparation and SEM of SiO_2−Pt−TiO_2 microrotors. Reprinted with permission from ref 27. Copyright 2011 American Chemical Society. (f) Trajectories of tadpole-shaped SiO_2−Pt−TiO_2 microrotors of different tail lengths (l). Reprinted with permission from ref 27. Copyright 2011 American Chemical Society.

likely because of an imperfect functionalization with enzymes that led to asymmetric propulsive forces parallel to the short axis of the rod.

3.2. Chiral Catalytic Microrotors ("100" and "110"). As shapes strongly affect the motion behavior of micromotors, a torque is expected to be introduced to micromotors if it is made into a chiral shape. Examples include nonaxisymmetric microrods,[67,77,83−87] tadpole-shaped microrotors,[24−28] chiral microgears,[29−33] "L"-shaped particles,[83,85] among others.

3.2.1. Microrotors of Chiral Rods. It is feasible to deform an entire microrod or one end of it using mechanical force because of their high aspect ratios, to create microrotors with broken axial symmetries. For example, Rao et al.[83] fabricated Au−Pt bimetallic microrods of an "L" shape by sonicating (thus breaking) a long straight fiber coated with Au and Pt layers (Figure 4a) ("110"). This L-shaped Au−Pt rod of an angle 105° moved in 5% H_2O_2 by self-electrophoresis and rotated at 0.29 rad/s. Liu et al.[77] electrodeposited copper (Cu) microrods in nanoporous alumina templates and broke the axi-symmetry of these rods into a crooked brush shape by mechanically polishing the bottom of the template (Figure 4b) ("100"). Because of the chiral shape, the Cu rod rotated at ∼18 rad/s in 0.2 mM Br_2 aqueous solutions.

Likewise, Wang et al.[84] prepared core−shell p−n junction nanowires shaped like syringe needles by mechanically scraping off nanowires from the wafer on which they were grown (Figure 4c) ("110"). In aqueous solutions of 1,4-benzoquinone/hydroquinone (Q/QH_2) or H_2O_2 and upon illumination, the negatively charged nanowires moved linearly toward the p-type silicon end via self-electrophoresis. As shown in Figure 4c, nanowires with a slanted tip due to imperfect fracture moved in circles, likely because of the now-broken axial symmetry of the distributions of ions around the nanowire. The sharper the tips were, the tighter the nanowire's trajectory became.

https://doi.org/10.1021/acsnano.2c11680
ACS Nano 2023, 17, 11969−11993

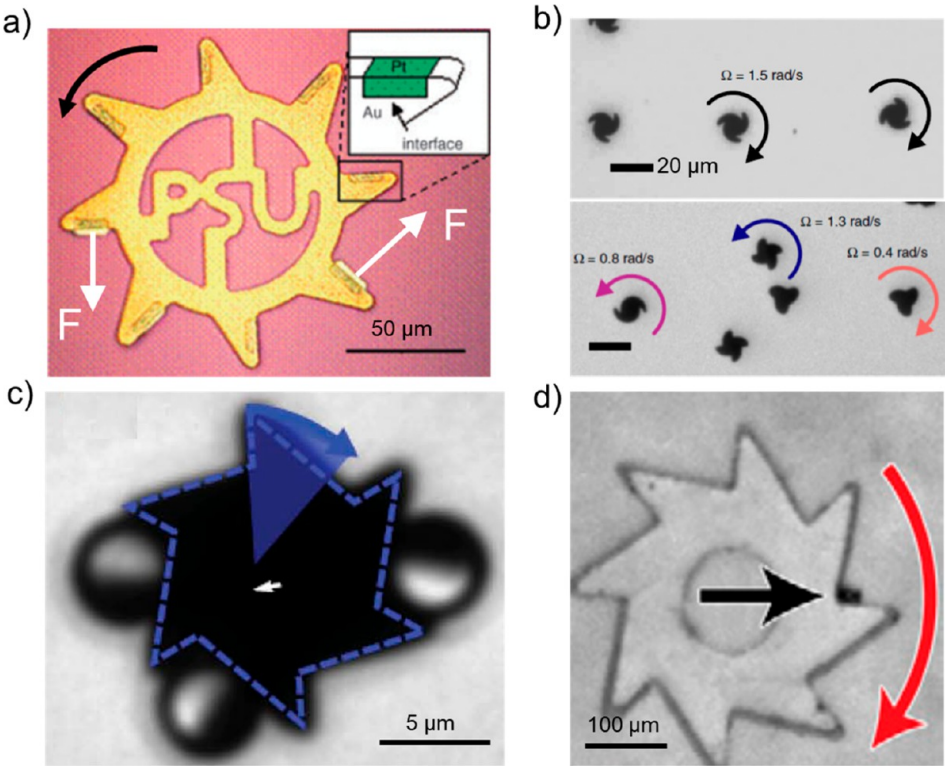

Figure 6. Microgear rotors ("100" and "110"). (a) Au microgear evaporated with Pt on one side of its teeth. Each tooth is thus made of a Au−Pt pair and powered by the electrochemical decomposition of H_2O_2. Reproduced with permission from ref 29. Copyright 2005 Wiley-VCH. (b) Pt microgears of different shapes rotate in different directions and at different angular speeds. Reproduced with permission under CC BY 4.0 from ref 30. Copyright 2019 Springer Nature. (c) Three SiO_2−Pt Janus particles dock in the gaps between the teeth of a SU-8 microgear with an external radius of 8 μm and rotate the gear. Reprinted with permission from ref 31. Copyright 2016 Wiley-VCH. (d) Rotation of a microgear made of SU-8 photoresist in a suspension of *Escherichia coli*. The arrow points to where the bacteria accumulate. Reproduced with permission from ref 32. Copyright 2010 National Academy of Sciences USA.

Although effective, using mechanical force to deform microrods often causes particle shapes to vary considerably, leading to inconsistent results. Alternatively, He et al.[85] fabricated L-shaped Si−Pt microrods precisely and controllably by GLAD (Figure 4d) ("110"). They began by depositing Si nanorods of 4 μm long at a large incident angle (>70°) to the normal of the sample stage. Then, a second segment of a 6-μm-long Si nanorods was deposited in the opposite direction by rotating the substrate 180°, to form an L-shaped Si nanorod. A final layer of Pt was then deposited on the second Si segment. In a solution containing 5% H_2O_2, the L-shaped Si rods rotated at 1.57 rad/s because of the catalytic decomposition of H_2O_2 by the Pt layer.

Microrods of varying diameters along their bodies can also be chemically synthesized. For example, Du et al.[67] used the hydrothermal method to synthesize ZnO microrods consisting of two sections of different diameters along the long axis, then sputtered a layer of Au on one side of the ZnO rod to form a heterojunction and to break the axial symmetry ("110"). Under UV illumination, the ZnO-Au microrod moved by self-electrophoresis in different motion modes in various concentrations of H_2O_2, including translation and rotation (Figure 4e). In a solution of 1% H_2O_2, it rotated at ∼7.5 rad/s. Zheng et al.[86] prepared photochemically driven core−shell $Zn_XCd_{1-X}Se$−Cu_2Se nanowires with uneven thickness along their axes and achieved on−off controlling of their orbiting motion (Figure 4f) ("110"). Zhang et al.[87] chemically synthesized Fe_2O_3@SiO_2 particles of matchstick shapes and physically deposited a layer of Pt that catalyzed the decomposition of H_2O_2, as shown in Figure 4g ("110"). This catalysis generated a driving force toward the uncoated SiO_2 side and made it rotate persistently.

3.2.2. Tadpole-Shaped Microrotors ("110"). Apart from breaking the symmetry of rod-shaped micromotors to generate rotation, combining a typical sphere micromotor with a microrod to prepare a tadpole-shaped microrotor can also effectively break its shape symmetry and lead to rotation. These tadpole-shaped microrotors can be prepared in a number of ways. For example, Lv et al.[24] prepared a tadpole-shaped microrotor consisting of a spherical "head" and a long silver nanowire "tail" by growing Ag out of a PS-Pt Janus microsphere (Figure 5a) ("110"). By controlling the length of the Ag tail, the rotational dynamics of this microrotor can be modulated in a controllable manner. For example, the curvature of its trajectory and angular speed both increase to the peak and then decrease as the Ag tail length increases (Figure 5b). In a solution of 1% H_2O_2, it reaches a maximum angular speed of ∼1.3 rad/s when the length of the Ag nanotail is about 13 μm. Similarly, Fattah et al.[25] selectively grew Pt particles on one side of a carbon microtube by bipolar electrochemistry, leading to microrotors of tadpole shapes (Figure 5c) ("110"). In a solution containing 30% H_2O_2, these microrotors can rotate at ∼3 rad/s driven by bubbles generated from the catalytic decomposition of H_2O_2 at the Pt surface.

Compared with chemical synthesis, physical vapor deposition prepares tadpole-shaped microrotors with higher precision. For example, Gibbs et al. used GLAD to prepare various tadpole microrotors, including a photochemically powered SiO_2−TiO_2−Au microrotors[26] (Figure 5d, "110"), and chemically

https://doi.org/10.1021/acsnano.2c11680
ACS Nano 2023, 17, 11969−11993

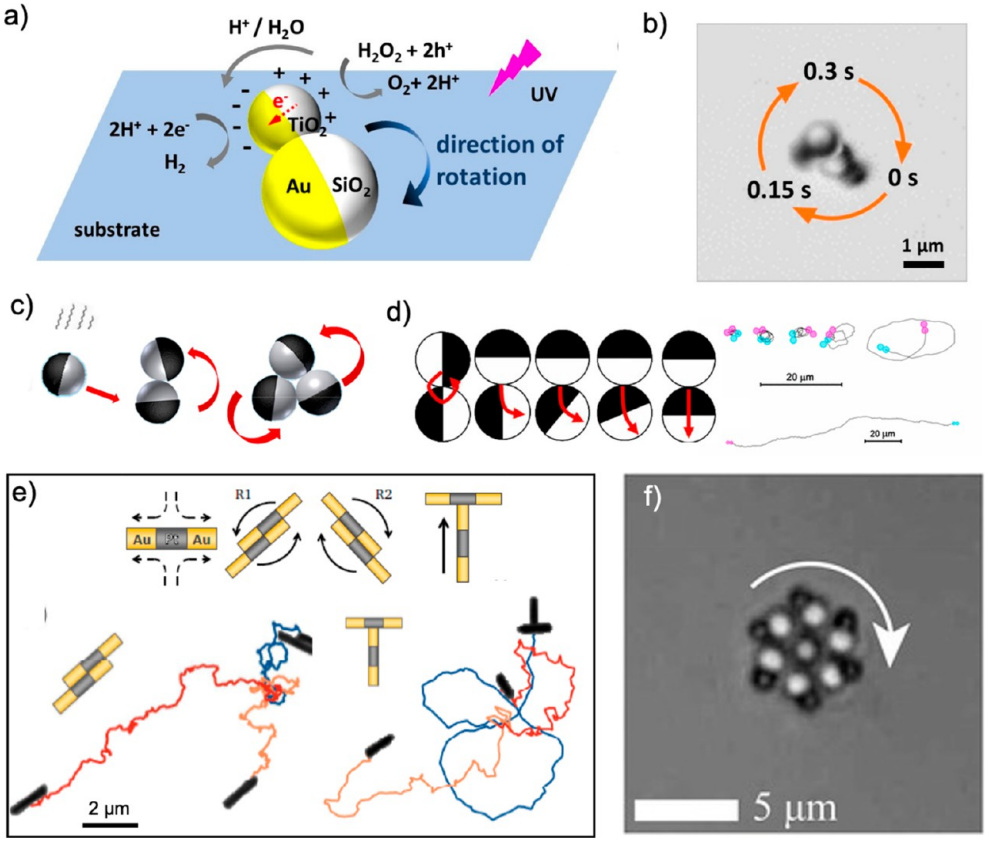

Figure 7. Rotating clusters ("010" and "110"). (a) Schematic and (b) overlaid optical micrographs of a snowman-shaped microrotor powered by H_2O_2 under UV light. Reproduced with permission from ref 53. Copyright 2021 Wiley-VCH. (c) Doublet and triplet microrotors made of SiO_2−Pt micromotors moving in H_2O_2. Reproduced with permission from ref 73. Copyright 2013 American Chemical Society. (d) Two Janus particles assembling into different configurations (left) and the corresponding trajectories (right). Reproduced with permission from ref 52. Copyright 2010 American Physical Society. (e) Schematic of trimetallic microrods (Au−Pt−Au) self-assembling into microrotors of different configurations and the corresponding trajectories. Reproduced with permission from ref 51. Copyright 2016 Royal Society of Chemistry. (f) Assembly of Janus microspinners into a rotating microgear. Reproduced with permission from ref 50. Copyright 2018 Royal Society of Chemistry.

powered SiO_2−Pt−TiO_2 (Figure 5e, "110") microrotors.[27,28] The fabrication starts with depositing a layer of Pt, Ti, or TiO_2 on a monolayer of SiO_2 microspheres to yield Janus particles. Then, a second layer of TiO_2 is deposited by tilting the substrate at an angle to produce a tadpolelike particle with the second layer acting like an arm. In particular, the radius of curvature of the trajectory of a SiO_2−Pt−TiO_2 microrotor decreases roughly linearly as the arm length increases (Figure 5f).

3.2.3. Rotating Microgears ("100", "110"). Microgears—microparticles with regularly spaced teeth that mimic macroscale gears—have also been used as microrotors and are attractive for their distinct shapes. By introduction of catalytic reactions asymmetrically on the gear teeth to generate driving force, a torque is created that drives rotation. Yang et al.[95] simulated a catalytic microgear that can rotate controllably through self-diffusiophoresis that arises from the catalytic reaction on the gear surface ("100"). This is echoed in a separate experiment, in which Catchmark et al.[29] fabricated by photolithography a Au microgear with Pt evaporated on its tooth (Figure 6a, "110"). In an aqueous solution containing peroxymonosulfuric acid, H_2O_2, and sulfuric acid, the gear rotated toward the Pt-coated side of the tooth at a high angular speed of ∼6.28 rad/s, because of the self-electrophoretic force generated by the electrochemical decomposition of H_2O_2 on each Au−Pt tooth. Similarly, Brooks et al.[30] fabricated by photolithography gear-like Pt microplates that rotated in H_2O_2 (Figure 6b, "100"). These Pt microgears were highly tunable in their shapes, such as chirality, fin numbers, curvature, and the distribution of teeth, and were thus good candidates for understanding the relationship between rotor shapes and their kinetics. For example, by tuning the shape asymmetry, these microplates could spin either clockwise or counterclockwise with angular speeds ranging from 0.4−1.5 rad/s in 10% of H_2O_2.

Another strategy to create microrotors is to make a passive microgear "active", by exposing it to motile micromotors or microorganisms. The idea is that motile microparticles can collide with a microgear and become trapped in the gaps among its teeth if the sizes of the particles and of the gaps are comparable. These motile particles then power the rotation of the gear of an asymmetric shape. For example, as shown in Figure 6c, Maggi et al.[31] used chemically powered SiO_2−Pt micromotors as the motile units to drive a microgear made of SU-8 photoresist into rotation at a maximum angular speed of ∼0.17 rad/s in a solution of 5% H_2O_2 ("110"). Alternatively, Leonardo et al.[33] and Sokolov et al.[32] immersed similar microgears in a bath of *Escherichia coli* and observed their rotation (Figure 6d, "110"). In this case, bacteria were stuck at the concave corners and, thus, pushed the microgear into rotation. In these cases, it is not the passive microgear by itself that is the rotor nor do the individual motile entities (e.g.,

https://doi.org/10.1021/acsnano.2c11680
ACS Nano 2023, 17, 11969−11993

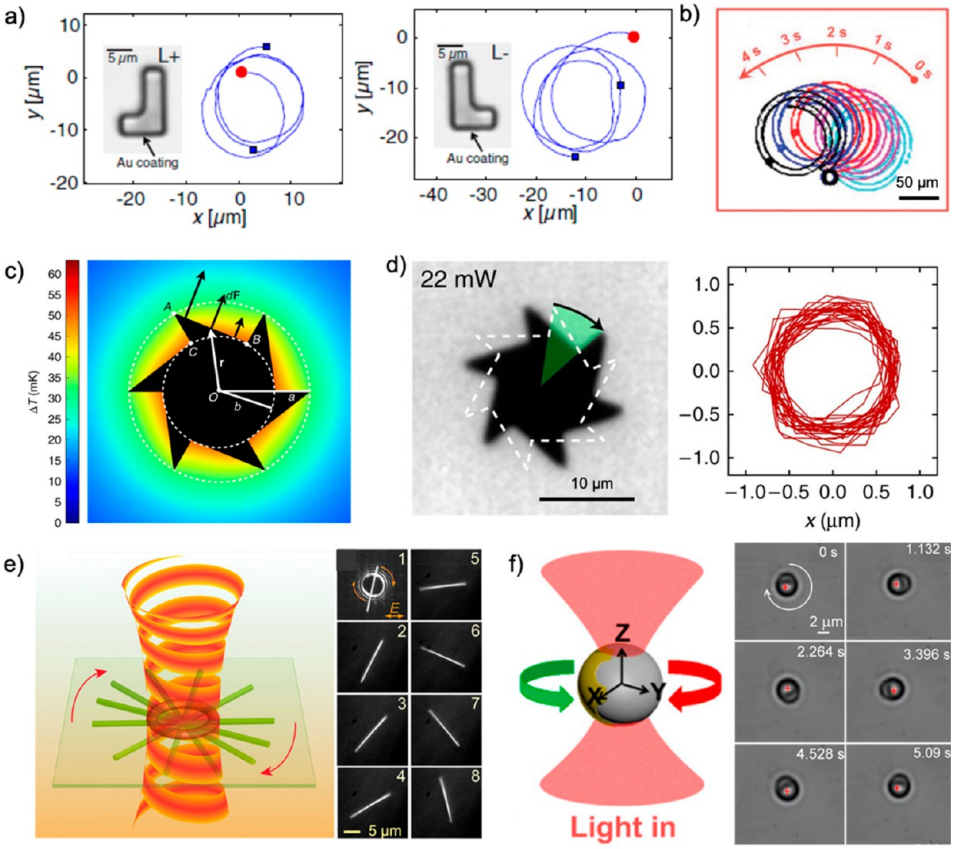

Figure 8. Microrotors powered by uniform light ("110", "100", and "001"). (a) Trajectories of L^+ and L^- microrotors. Inset: SEM images of two types of L-shaped microrotors. Reproduced with permission from ref 34. Copyright 2013 American Physical Society. (b) Overlaid images of a spiral microgel rotor tethered to a sphere. Reprinted with permission under CC BY 4.0 from ref 78. Copyright 2019 Wiley-VCH. (c) A temperature gradient around a microgear generates asymmetric surface tension forces, rotating the microgear. (d) Optical image of a microgear showing the rotational displacement in a time interval of 20 ms at light power of 22 mW (left) and the corresponding trajectories of the gear center for a time interval of 5 s (right). (c,d) Reprinted with permission under CC BY 4.0 from ref 88. Copyright 2015 Springer Nature. (e) Illustration (left) and time-lapsed images (right) of a rotating Ag nanowire for a time interval of ~0.5 s (right). Reproduced with permission from ref 61. Copyright 2013 American Chemical Society. (f) Illustration (left) and snapshots (right) of a rotating PS-Au Janus microsphere upon illumination with linearly polarized light. Reproduced with permission from ref 101. Copyright 2015 American Chemical Society.

bacteria or artificial micromotors). Rather, it is the combination of the autonomous translators and the passive gear with the motors arranged in an appropriate way that collectively constitutes a microrotor.

3.3. Rotating Clusters ("010", "100", "110", "111"). Grouping a few micromotors together often introduces torques that rotate the resulting cluster. Following our naming convention, the rotating cluster can be a "100" rotor (a chiral cluster containing constituents that are isotropic and achiral), a "110" cluster (one containing chiral constituents),[49,51] or a "010" cluster (an achiral cluster made of Janus microspheres, for example).[51−53,73]

Lv et al.[53] synthesized snowman-shaped microrotors made of one small TiO_2-Au and one large Au-SiO_2 microsphere, as shown in Figure 7a,b ("010"). Under UV light, the microrotor moved persistently via self-electrophoresis arising from photocatalysis on the surface of TiO_2-Au microspheres in H_2O_2. They rotated because of the shape and chemical asymmetries. Gao et al.[73] reported rotating clusters containing octadecyltrichlorosilane-modified silica microspheres half-coated with Pt, as shown in Figure 7c ("010"). These spheres clustered via hydrophobic interactions. Even achiral clusters assembled in this way could rotate stably in H_2O_2 because of the asymmetric distributions of the catalytic Pt caps in the cluster.

Rotating clusters can also be assembled by phoretic interactions among micromotors. For example, Ebbens et al.[52] systematically studied the dynamics of doublets formed by the self-assembly of PS-Pt Janus microspheres in H_2O_2, as shown in Figure 7d ("010"). They discovered that the resulting cluster moved in straight lines if made of two spheres with their Pt caps pointing in the same direction while rotating if the Pt caps point to different directions. The radius of a cluster's trajectory is also sensitive to the orientation of each Pt cap. In a later study, Wykes et al.[51] found that trimetallic microrods (Au−Pt−Au) were immotile but self-assembled into rotating clusters of various configurations (Figure 7e), with an angular speed of 1.3−6.3 rad/s in 3% H_2O_2 ("110", "010"). More recently, Aubret et al.[49,50] reported spinning microgears self-assembled from a dimer made of a hematite cube fused into a polymer sphere (Figure 7f, "110"). These dimers moved autonomously under light via self-diffusiophoresis and assembled toward a laser spot into a rotating cluster of well-defined shapes and chirality. The assembly was believed to be due to the torque on the polymer sphere by the hematite cube undergoing negative phototaxis.

4. EXTERNAL FIELD DRIVEN MICROROTORS

There has been significant effort to realize the controllable rotation of microrotors driven by external fields (e.g., magnetic,

https://doi.org/10.1021/acsnano.2c11680
ACS Nano 2023, 17, 11969−11993

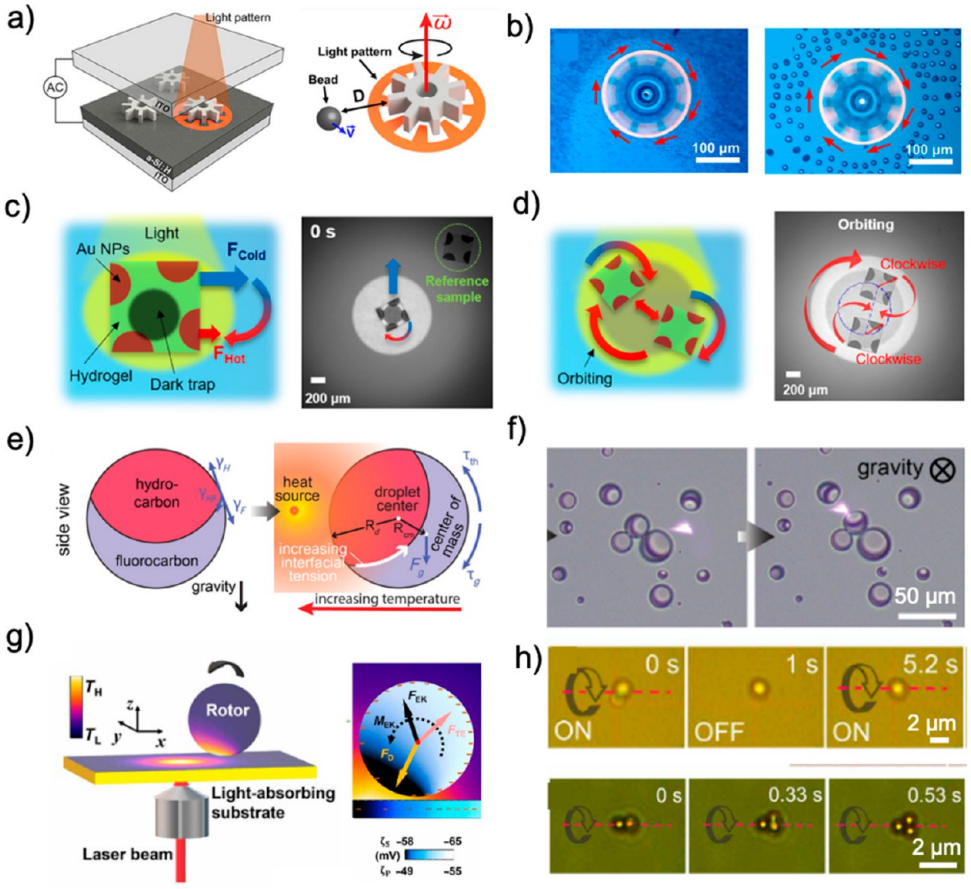

Figure 9. Microrotors rotated by light patterns. (a) Schematic of the optoelectronic tweezer (OET) device (left) and a rotating microgear of angular velocity ω (right) in the device. (b) A microgear rotating at 2π rad/s in a suspension of polystyrene microbeads (Left: 1 μm in diameter. Right: 15 μm in diameter). (c) Schematic (left) and optical image (right) of a square-shaped hydrogel spinner containing chiral Au nanoparticles patterns. (d) Schematic (left) and optical image (right) of two square-shaped hydrogel spinners orbiting in a circular light well. (e) Schematic and (f) time-lapsed images of the Janus emulsion droplets rotating toward the heat source. (g) Schematic of the experimental setup (left) and working mechanism (right) for the OTER of micro/nanoscale rotors. (h) Successive optical images of a rotating dimer composed of two 2-μm silica particles (top) and trimer composed of three 1-μm PS particles (bottom). (a,b) Reproduced with permission from ref 63 which are licensed under CC BY 4.0. Copyright 2021 Springer Nature. (c,d) Reproduced with permission from ref 104. Copyright 2021 National Academy of Sciences USA. (e,f) Reproduced with permission from ref 105. Copyright 2021 American Physical Society. (g,h) from ref 64. Copyright The Authors, some rights reserved; exclusive licensee AAAS. Distributed under a CC BY-NC 4.0 license http://creativecommons.org/licenses/by-nc/4.0/. Reprinted with permission from AAAS.

electric, light, or ultrasound). Compared with catalytic microrotors, those powered by external fields are amenable to more precise, on-demand control of their rotational speeds and directions. Externally powered microrotors have the additional advantages of being fuel-free, often more biocompatible than catalytic microrotors, and usually capable of generating greater propulsive forces. These advantages bode well for their implementation in biomedical applications. In the following section, microrotors powered by light, magnetic field, electric field, and ultrasound are discussed in detail.

4.1. Light-Driven Microrotors. Light as a power source has many benefits to drive microrotors. For example, it generally requires less complicated equipment to generate, and it is generally easier to tune its intensity, polarization, wavelength, incident direction, and spatiotemporal distributions.[86,96−99] Broadly speaking, light-driven microrotors are divided into two categories. One is photochemically powered microrotors, in which the light induces a chemical reaction on the particle surface that drives rotation, which we regard in this review as a subtype of catalytic microrotor elaborated on in section 3. The second type does not involve any chemical reaction, but rather takes advantage of photothermal effect, optoelectronic tweezers, opto-thermoelectric effect, or the angular momentum of photons, and is what we mainly discuss in this section.

4.1.1. Microrotors under Uniform Light Intensities ("110" and "100"). One popular way of using light to power microrotors is to establish a temperature gradient by the photothermal effect. For example, Kümmel et al.[34] prepared L-shaped microrotors with two configurations (denoted as L^+, L^-) using photolithography (Figure 8a, "110"). In a homogeneous mixture of water and 2,6-lutidine, a local phase separation of the solvent is induced due to the photothermal effect by Au coating on the front side of the short arm under the illumination of 532 nm light. Then, the self-phoretic force derived from the asymmetric distribution of the lutidine molecules rotates the microrotors either clockwise or counterclockwise. Zhang et al.[78] reported a spiral-shaped microgel consisting of poly(N-isopropylacrylamide) (PNIPAM) embedded with gold nanorods, which rotated by nonreciprocal curling deformations when illuminated with near-infrared light (Figure 8b, "100"). Maggi et al.[88] also used photolithography to fabricate microgears coated with a uniform layer of amorphous carbon on one side (Figure

https://doi.org/10.1021/acsnano.2c11680
ACS Nano 2023, 17, 11969−11993

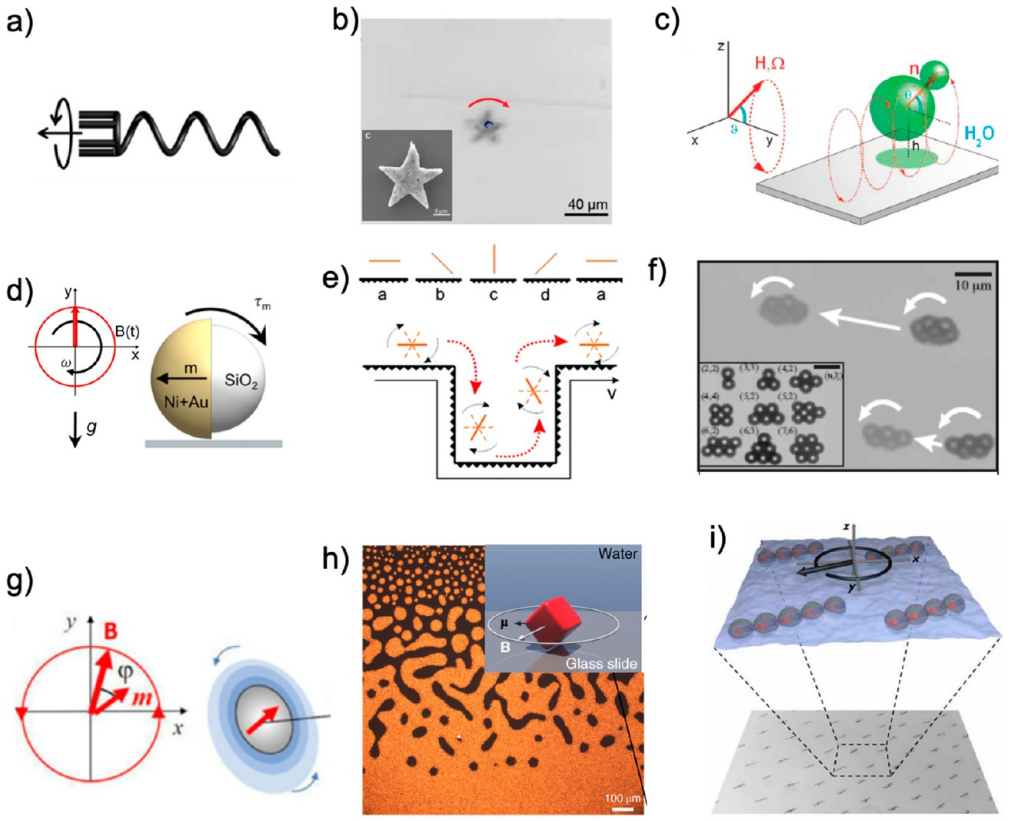

Figure 10. Magnetically powered microrotors. (a) Drilling of a helix under rotating magnetic field. Reprinted with permission from ref 56. Copyright 2012 Wiley-VCH. (b) Rolling of a star-shaped hydrogel modified by Fe_3O_4 nanoparticles. Inset: SEM of the star-shaped hydrogel. Reproduced with permission from ref 112. Copyright 2018 Wiley-VCH. (c) Rotating doublet made of paramagnetic particle. Reproduced with permission from ref 36. Copyright 2008 American Chemical Society. (d) Schematic of a rolling SiO_2–Ni–Au microsphere in a uniform rotating magnetic field. Reproduced with permission under CC BY 4.0 from ref 113. Copyright 2021 National Academy of Sciences USA. (e) A Ni nanowire crosses the microchannel via tumbling motion. Reproduced with permission from ref 68. Copyright 2010 American Chemical Society. (f) Translation of 5-mer and 7-mer rolling microwheels. Inset: μwheels with different size. Reproduced from ref 70. Copyright 2019 American Association for the Advancement of Science. (g) Schematic of the in-plane spinning of a ferromagnetic hematite ellipsoid in a rotating magnetic field. Reproduced with permission under CC BY 4.0 from ref 116. Copyright 2021 American Physical Society. (h) Patterns formed by magnetically spinning hematite microcubes. Reproduced with permission from ref 117. Copyright 2019 Springer Nature. (i) Self-assembled magnetic spinners at an air–water interface, from ref 118. Copyright The Authors, some rights reserved; exclusive licensee AAAS. Distributed under a CC BY-NC 4.0 license http://creativecommons.org/licenses/by-nc/4.0/. Reprinted with permission from AAAS.

8c,d, "110"). The asymmetric thermocapillary flows induced by the heating of the microgear rotate it at up to ∼31 rad/s at an air–liquid interface.

4.1.2. Microrotors Enabled by the Angular Momentum of Photons ("001", "101", or "011"). Beth et al. discovered in 1936 that the angular momentum carried by photons can be directly used to rotate microparticles.[100] This phenomenon has in recent years been used to drive the controlled rotation of microrotors by light. For example, Yan et al.[61] rotated a single Ag nanowire by transforming the orbital angular momentum of linearly polarized optical vortices (Figure 8e, "001"). Because of the strong plasmonic interactions between Ag nanowires and light, the angular speed of a Ag nanowire is nonuniform in different orientation within a circle, with a maximum of ∼6 rad/s under the irradiation of light with a power of 100 mW. Zong et al.[101] realized the rotation of a PS-Au Janus microsphere in a focused linearly polarized optical trap ("001"). By changing the light intensity and the position of the laser beam, both the angular velocity and the rotational direction of PS-Au microrotors can be precisely controlled (Figure 8f). More examples of using the angular momentum of light to drive microrotors include micro turbine ("001"),[102] Au nanoparticles[62] ("001"), carbon nanotube bundles[60] ("001"), SiO_2 microdisk[35] ("001"), microdrone[48] ("011"), and metavehicles[47] ("101").

4.1.3. Microrotors Rotated by Structured Light ("001" and "010"). Switching light illumination from being uniform to being structured can make things move at microscopic scales,[99,103] as well as to rotate them. For example, Zhang et al. prepared via photolithography a microgear with a hole in its center and eight teeth that were arranged symmetrically ("001"). By rotating the light pattern, the microgear exhibited controllable rotation in a system called "optoelectronic tweezers" (OET) (Figure 9a, b).[63] Using a different approach, Kim et al. prepared a square hydrogel disk embedded with four off-centered semicircular patterns of Au nanoparticles. Upon uniform illumination, the surface plasmon resonance of these Au nanoparticles generated a temperature gradient across the disk, and the resulting surface tension gradient on the air–water interface spins the disk (Figure 9c). Moreover, the disk can switch from spinning to orbiting by tuning the light patterns (Figure 9d).[104] The last two examples are classified as 010 rotors because their rotation is directly caused by the asymmetric placement of the metal patches; since the incident light that powers the motion is

https://doi.org/10.1021/acsnano.2c11680
ACS Nano 2023, 17, 11969–11993

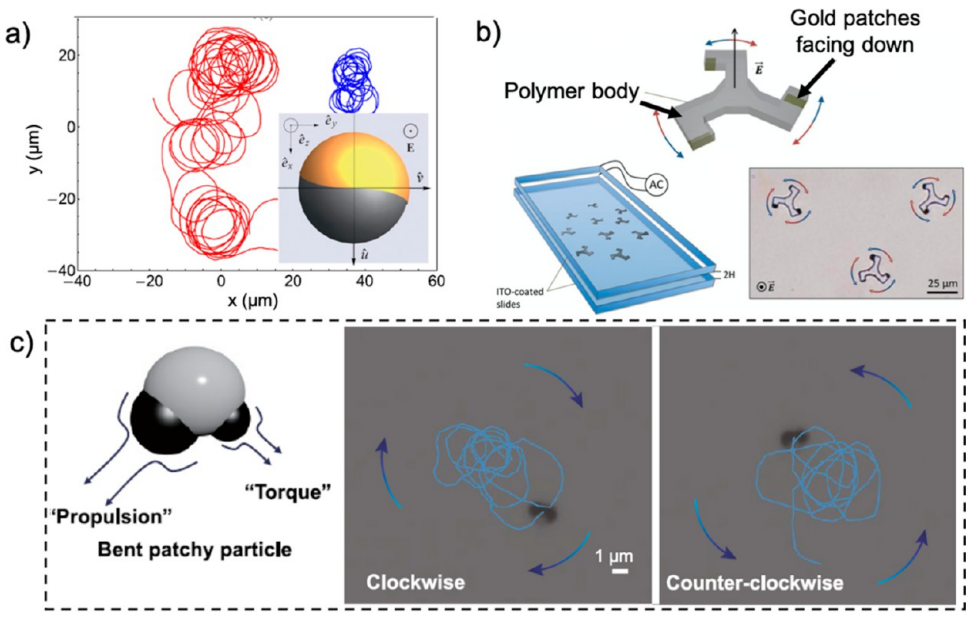

Figure 11. Singular microrotors powered by uniform electric fields ("010" and "110"). (a) Rotation of a PS-Au Janus particle undergoing ICEP at different angular speed. Inset: Illustration of a PS-Au Janus sphere with an uneven Au cap. Reproduced with permission from ref 120. Copyright 2017 National Academy of Sciences USA. (b) Schematic illustration of the electrically switchable spinning of a microgear made of a polymer body and gold patches on its teeth. Reproduced with permission from ref 79. Copyright 2018 Wiley-VCH. (c) Trajectories (right) of a bent patchy particle (left) driven by ICEP under AC electric fields. Reproduced with permission from ref 38. Copyright 2019 American Chemical Society.

uniform and does not cause rotation directly, a "0" is inserted in the third spot.

In addition to complex light patterns, a laser beam can also effectively rotate microrotors, serving as a localized heat source. For example, making use of the Marangoni force that was induced by the temperature gradient, Nagelberg et al. rotated a Janus emulsion droplet made of hydrocarbon and fluorocarbon toward a laser spot (Figure 9e,f, "001").[105] Ding et al. developed opto−thermoelectric rotation (OTER), where microscopic objects rotated by a laser beam that locally heated a substrate (Figure 9g,h, "001").[64] Briefly, nonuniform illumination generates a temperature field on a specialized surface that is functionalized with a self-assembled monolayer of carboxylic acid-terminated alkanethiol. Because carboxylic acids tend to dissociate more easily in regions of lower temperatures, this temperature gradient leads to charge distributions on the substrate, which ultimately leads to an electrostatic torque that rotates charged colloidal particles. Microrotors of different sizes, shapes, and compositions were realized by this effect, including SiO_2 and PS microspheres, PS-Au Janus spheres, dimer, trimer, and hexamers composed of SiO_2 and PS microspheres.

4.2. Magnetic Microrotors. There is mounting interest in magnetic field-driven microrotors because of the biocompatibility and excellent controllability of a magnetic field.[106−108] The driving mechanism of magnetic-dipole-induced microrotors is shown in Figure 2. The magnetic dipole moment (**m**) of magnetizable particles tends to align with the direction of the external magnetic field that induces **m**. Thus, when the direction of the magnetic field changes, the resulting misalignment of **m** and the field causes a torque on the particle that tends to align the dipole and field. Magnetic microrotors typically require a nonuniform or time-varying magnetic field. Because the magnetic field is the proximate cause of their rotation, these rotors are classified as 001.

A common way to induce rotation is to expose a magnetic particle to a magnetic field rotating about an axis parallel to the bottom substrate. A magnetic helix illustrated in Figure 10a is one example,[56] which was introduced by Ghosh and Fischer[57] and is now being adapted for applications involving penetration of hyaluronan gels,[109] mucin gels,[110] and tissues such as the vitreous body of the eye.[111] Note that their helical shapes are not necessary for their rotation but only needed to convert rotation into linear motion, so that they are still 001 rotors by our definition. Although these helices are technically "microrotors", they are mostly studied as micromotors that move linearly, which fall outside of the scope of this review.

Similar strategies that use a rotating magnetic field have been applied to drive a variety of magnetic microrollers, such as a star-shaped hydrogel modified by Fe_3O_4 nanoparticles[112] (Figure 10b), magnetic (Janus) microspheres[36,113,114] (Figure 10c,d), microrods[68] (Figure 10e), and assemblies of magnetic (Janus) microspheres[70,114,115] (Figure 10f). In these cases, the microrotors roll above a boundary, because of the different frictional forces experienced by the rotor between its top and the bottom surface that is typically no-slip.[114] Based on this strategy, a variety of functions have been designed for these "rollers". For example, Zhang et al.[68] controlled a Ni microrod to cross a microchannel using a rotating magnetic field, greatly enhancing the ability of a microrobot to move on complex solid surfaces (Figure 10e). Torres et al.[69] used a Ni microrod to push or pull an inert magnetic microsphere. Alapan et al.[44] used rotating magnetic spheres for cargo delivery. Yang et al.[70] fabricated microwheels of various structures that roll on topographic surfaces with enhanced speeds (Figure 10f).

Another type of magnetic microrotor spins in place under a magnetic field rotating about an axis perpendicular to the bottom substrate. For example, Massana-Cid et al. demonstrated that spinning ferromagnetic hematite ellipsoids collectively organized into separated circulating clusters via

https://doi.org/10.1021/acsnano.2c11680
ACS Nano 2023, 17, 11969−11993

hydrodynamic and dipolar interactions (Figure 10g).[116] Soni et al. showed that millions of 1.6 μm hematite colloidal cubes spinning under a rotating magnetic field spontaneously formed a two-dimensional chiral liquid (Figure 10h).[117] Ferromagnetic nickel (Ni) particles spinning on an air−water interface by a rotating magnetic field were found to assemble into a lattice of synchronized spinners (Figure 10i).[118] More examples of the collective behaviors of magnetic spinners and rollers are discussed in section 5.3.

4.3. Electric Field-Driven Microrotors. In addition to magnetic fields, electric fields are another common power source for driving microrotors. In most cases, strategies "010", "110", and "001" are commonly employed to realize electrically powered microrotors.

4.3.1. Individual Microrotors Driven by Electric Fields ("010" and "110"). Microparticles exhibit a wide range of electrokinetic phenomena,[119] such as electrophoresis, induced-charge electrophoresis (ICEP), and dielectrophoresis (DEP). Using these electrokinetic phenomena, microparticles of specialized designed electrical properties can rotate controllably in an electric field. For example, Mano et al.[120] found that PS-Au Janus microspheres rotated under alternative current (AC) electric field via ICEP, possibly because Au was deposited nonuniformly ("010"). As shown in Figure 11a, the edge between Au and PS is not perfectly straight, which breaks the axis-symmetry of this microsphere. The resulting induced-charge electroosmosis (ICEO) flow then becomes unbalanced, inducing a torque on the sphere and rotating it. Shields et al.[79] designed a chiral microgear made of polymer consisting of three teeth partially deposited with gold (Figure 11b, "110"). As the AC frequency increased from 0.1 to 70 kHz, the microgear underwent two transitions of rotation direction from clockwise to counterclockwise, respectively, because it was believed to have gone through stages of electrohydrodynamics (EHD), inverse EHD, ICEP, and self-dielectrophoresis (sDEP) as the frequencies increased. At an electric field frequency of 0.1 kHz, it reached a maximum angular speed of ~2.4 rad/s. Wang et al.[38] fabricated a patchy particle consisting of a polymer sphere made of 3-(trimethoxysilyl)propyl methacrylate (TPM) and two gold patches of different sizes that were arranged asymmetrically (Figure 11c, "110"). Under an AC electric field, the ICEP force was asymmetric on the particle, generating a torque that rotated it. By modulation of the exact position of the two metal patches, the particle could rotate either clockwise or counterclockwise.

4.3.2. Rotating Doublets or Clusters in Electric Fields ("010" and "110"). Sustained rotation has been observed for doublets and clusters of catalytic PS-Pt Janus microspheres in H_2O_2,[52] and similar rotation was also found for Au-PS (metal−dielectric) Janus micromotors under an electric field. As shown in Figure 12a, PS-Au microspheres that move linearly under the AC electric field spontaneously self-assemble into doublets due to dipole−dipole interactions as they become close to each other. The formed doublets rotated because the metal−dielectric interfaces of the two spheres were not aligned symmetrically, leading to an asymmetry of the driving force (ICEP force)[76] ("010"). Similarly, SiO_2−Ti Janus microspheres can assemble into a three-arm pinwheel rotating clockwise in a solution of 0.1 mM NaCl under an AC electric field of 400 kHz, 40 V/mm (Figure 12b)[90] ("110"). Ma et al.[91] transformed translational snowman-shaped particles into rotational clusters using EHD flow under an AC electric field of ~600 Hz, as shown in Figure 12c ("110"). Ni et al. linked microspheres of different materials into hybrid clusters via sequential capillarity-assisted particle assembly, and the resulting clusters rotated by asymmetric electrohydrodynamic flows[89] (Figure 12d) ("110").

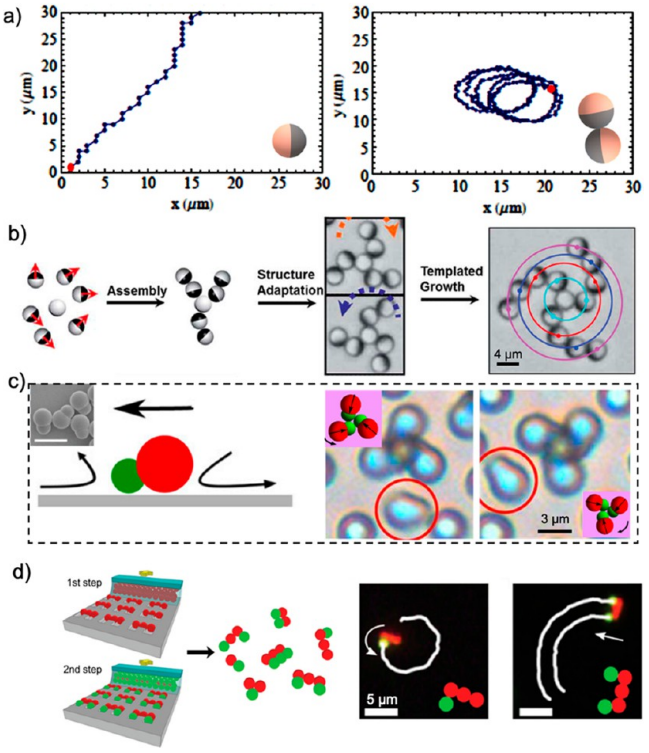

Figure 12. Agglomerate electric field-driven microrotors ("010" and "110"). (a) Trajectories of PS-Au micromotor (left) and their self-assembled doublets (right) under AC electric field. Reproduced with permission from ref 76. Copyright 2014 American Physical Society. (b) Schematic of the growth of a three-arm symmetric pinwheel rotating clockwise. Reproduced with permission from ref 90. Copyright 2016 Royal Society of Chemistry. (c) Schematic showing that the EHD flow can propel a snowman-shaped microparticle and cause a chiral cluster to rotate. Inset (left): SEM image of the snowman-shaped microparticles. Scale bar: 5 μm. Inset (middle and right): Optical micrographs of chiral clusters made of snowman-shaped microparticles. Reproduced with permission from ref 91. Copyright 2015 National Academy of Sciences USA. (d) Clusters formed by sequential capillarity-assisted particle assembly rotate via electrohydrodynamic flows. Reproduced with permission from ref 89. Copyright 2017 Royal Society of Chemistry.

4.3.3. Microrotors Enabled by Electric Dipoles ("001"). Similar to a rotating magnetic field, rotating electric fields can also rotate a micromotor controllably and at ultrahigh speeds. For example, Kim et al.[39] created a rotating electric field with a quadruple microelectrode of the same magnitude and frequency but a sequential 90° phase shift on each electrode (Figure 13a, "001"). Metallic nanowires, as well as semiconductor and insulating nanowires such as Si (Figure 13b) and SiO_2, can align and rotate with the rotating AC electric fields.[40,65] In 2014, Kim et al. used the same method to realize ultrahigh speed rotation at over 1884 rad/s for Au/Ni/Au metallic nanowires magnetically anchored onto a nanodisk[66] ("001").

Quincke rollers are another type of microrotors enabled by the interactions of electric dipoles with an electric field.[121−125] An opposite electric dipole moment **p** is induced in a dielectric sphere placed in an organic solution (typically hexadecane) and subjected to a vertical direct current (DC) electric field E. Once the electric field strength reaches above a critical point, the

https://doi.org/10.1021/acsnano.2c11680
ACS Nano 2023, 17, 11969−11993

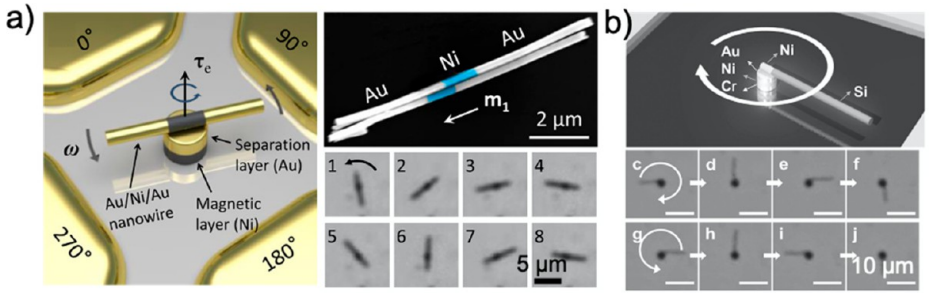

Figure 13. Microrotors enabled by electric dipoles ("001"). (a) Schematic of a Au/Ni/Au nanowire rotating under a rotating electric field enabled by quadrupole electrodes (left). SEM image and snapshots of the rotating Au/Ni/Au nanowire (right). Reproduced with permission from ref 39. Copyright 2015 American Chemical Society. (b) Schematic (top) and snapshots (bottom) of a rotating Si nanowire under a rotating electric field. Scale bar in snapshots: 10 μm. Reproduced with permission from ref 65. Copyright 2014 Wiley-VCH.

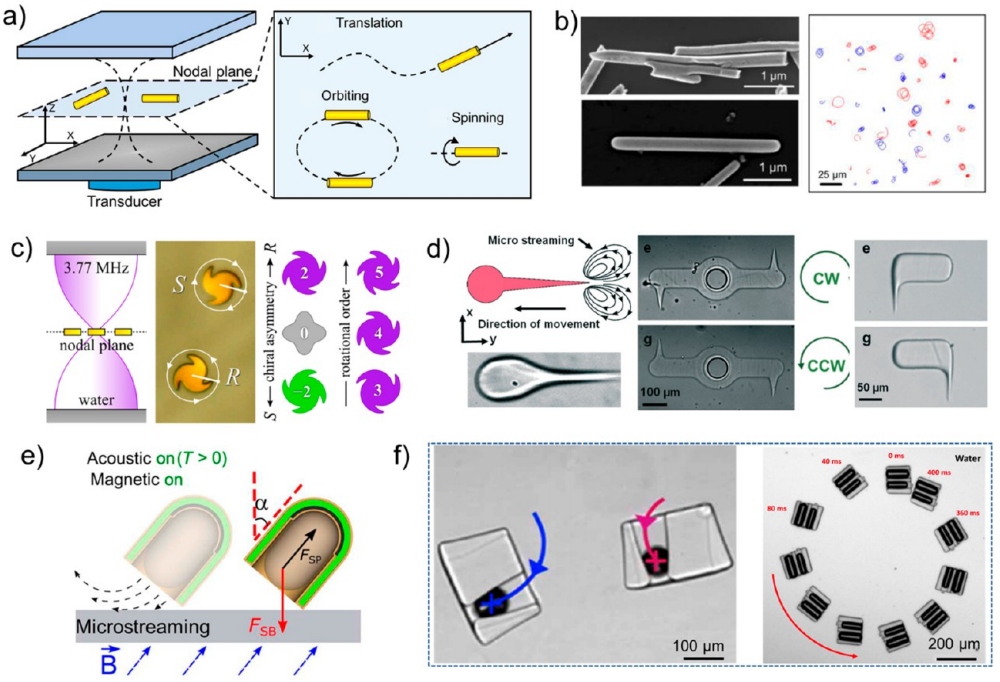

Figure 14. Ultrasonically powered, geometrically asymmetric microrotors ("100"). (a) Illustration of three kinds of motion (translation, spinning, and orbital motion) of metal nanorod on the nodal plane. Reproduced with permission from ref 41. Copyright 2017 American Chemical Society. (b) (Left) SEM of Au nanorods (top) fabricated by electrodeposition and Ag nanorods (bottom) with perfect shape symmetry. (Right) Trajectories of Au nanorods orbiting on the nodal plane. Reproduced with permission from ref 41. Copyright 2017 American Chemical Society. (c) Schematic of microgears with different chirality spinning on the nodal plane. Reproduced with permission from ref 46. Copyright 2018 American Chemical Society. (d) Schematic of microstreaming generated on the tip of the microstructure (left). Optical images of flagellated microrotors with different chiralities and their rotational directions (middle and right). Reproduced with permission from refs 81, 136. Copyright 2016 and 2017 Royal Society of Chemistry. (e) Schematic of the generation of a streaming propulsive force arising from the resonance of a bubble trapped in a microcapsule, from ref 137. Copyright The Authors, some rights reserved; exclusive licensee AAAS. Distributed under a CC BY-NC 4.0 license http://creativecommons.org/licenses/by-nc/4.0/. Reprinted with permission from AAAS. (f) Rotation of two microrotors carrying one bubble each (left) and the overlaid snapshots of a microrotor containing two bubbles (right). Reproduced with permission under CC BY 4.0 from ref 82. Copyright 2015 Springer Nature.

resulting **p** becomes unstable, and the spontaneous deviations between **E** and **p** produce a net torque that rotates the polarized microsphere. In the presence of a substrate, the spinning dielectric sphere rolls forward.[122] As a microrotor, the Quincke roller is a rare exception to our naming convention because although the electric field is necessary for breaking the rotational symmetry, it does so in an indirect and subtle way. This is very different from all of the other rotor examples we described in the current article that have "1" at the last digit, which requires the energy field to be directly responsible for the rotor's rotation. As the 3-digit index is defined, the Quincke roller would *not* have a "1" in any of the three positions. The proximate cause of rotation in this case is the interaction between the electric field and the electrical dipole moment vector of the microspheres, which leads to a torque.

Quincke rollers are suitable model systems for active microrotor systems due to their simple fabrication, clean working environment (without any chemical reaction), good controllability, and well-defined driving mechanism. Recent studies of Quincke rollers have discovered a wide range of interesting dynamics, including the motion behavior of rollers with ellipsoidal shapes,[126] drops,[127] a bead-flagella dimer,[128] the nontrivial emergent dynamical phenomena in pulsating electric field[129] and in the subcritical regime where one isolated particle

https://doi.org/10.1021/acsnano.2c11680
ACS Nano 2023, 17, 11969−11993

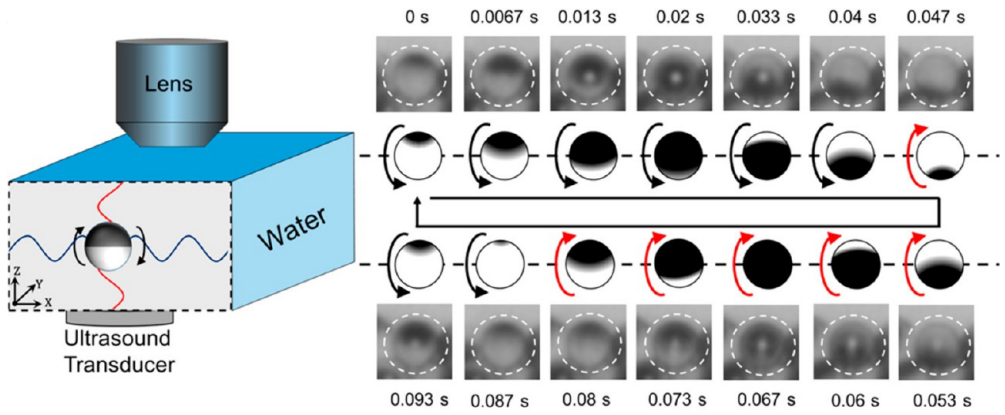

Figure 15. Microrotors rotated by nonuniform ultrasound ("001"). Schematic (left), snapshots (right), and cartoon illustration (right) of a SiO_2−Ti Janus microsphere spinning on the nodal plane formed by two orthogonal standing acoustic waves. Reproduced with permission from ref 41. Copyright 2017 American Chemical Society.

cannot move,[130] and the interaction between Quincke rollers with complex environments.[123,125,131]

4.4. Ultrasonically Driven Microrotors. Ultrasound has been widely applied for biomedical imaging because of its strong penetration ability and noninvasive nature.[132,133] In the fluid, localized microstreaming will be generated around a rigid topological feature that is driven into oscillation under an external acoustic field.[81,134] By designing microstructures appropriately, various motion modes, e.g., translation, spinning, orbiting, of micro-objects driven by acoustic fields can be obtained.

4.4.1. Microrotors under Uniform Ultrasound ("100"). Many ultrasonically driven microrotors are powered by ultrasound generated by a substrate that, as far as a small observation region is concerned, is vibrating at the same amplitude and phase everywhere. In this case, strategy "100" is most popular in designing ultrasonically driven microrotors of chiral particle shapes.

For example, Wang et al.[42] discovered in 2012 that resonating megahertz ultrasound (~3.7 MHz) could drive metal nanorods into three distinct modes of motion on an acoustic nodal plane: translation, spinning, and orbiting (Figure 14a). A mechanism of growing popularity is centered around microstreaming, in which a net streaming flow is generated along the axis of the rod due to its asymmetric shape under ultrasound, propelling it toward its concave end.[43,80] However, this can explain only its translation, not rotation. In 2017, Zhou and Zhao et al. found that the metal microrods synthesized by electrodeposition are slightly curved (Figure 14b, left), which leads to an uneven distribution of acoustic forces and torques, leading to the orbital motion of the rods (Figure 14b, right, "100").[41] Silver nanorods with perfect shape axis-symmetry, on the other hand, did not translate or orbit on the plane, lending support to this argument of shape asymmetry.

The shape of a microparticle also plays an important role in inducing spinning. Similar to the work in Figure 14c, Sabrina et al.[46] fabricated gear-like Au microplates that rotated on a nodal plane in megahertz ultrasound ("100"). By adjusting their chiral asymmetry and fin number, both clockwise and counterclockwise rotation were found. In addition, the angular speeds of these microplates were modulated by changing their sizes, independent of the fin number. Very recently, McNeil et al. fabricated microdisks with chiral arms that spontaneously spin (with controlled chirality) in ultrasound ("100").[135] Interesting collective behaviors, such as 3D assembly and phase separation, were reported.

Strong microstreaming is also generated at an oscillating tip and moves a microswimmer with such a tip tail linearly in the acoustic field, as shown in Figure 14d, left. By rationally designing the position and number of the tip on a microswimmer, an acoustic field driven microrotor can be obtained. For example, Kaynak et al.[81,136] prepared a microrotor with two sharp tails and a flagellated microrotor, respectively, as shown in Figure 14d ("100"). Upon acoustic excitation, asymmetric streaming flows is generated because of the oscillation of a sharp tail, rotating the particle clockwise or counterclockwise depending on the chirality of the particle shape.

Localized microstreaming can be also formed by the resonance of bubbles trapped in a microcapsule, which will generate a streaming force that is in turn exerted on the microcapsule[137] (Figure 14e). For example, Ahmed et al.[82] fabricated an acoustically powered microswimmer propelled by the oscillation of bubble that is trapped in its hydrophobic cave, as shown in Figure 14f ("100"). By tuning the position, number of bubbles, and relative size between bubbles, stable rotation of these microrotors with specific rotational modes, such as spin or orbiting, can be achieved.

4.4.2. Microrotors Rotated by Nonuniform Ultrasound ("001"). Nonuniform ultrasound can also effectively rotate microparticles. For example, Wang et al.[41] reported the spinning of SiO_2−Ti, PS, SiO_2 microspheres (Figure 15), and perfectly axisymmetric cylindrical Ag nanorods on an acoustic nodal plane. Even though some of the particles (the Janus particles) have asymmetric surface patterning, the patterning is not necessary for a torque to be induced, and thus, they are all classified as "001" rotors. The mechanism for spinning is believed to be related to the phase difference of sound waves propagating in the *X*, *Y*, and *Z* directions, which induce surface acoustic streaming and generate torque on microparticles of symmetric shapes. Such orthogonal acoustic fields could arise from sound scattering from side walls of an experimental chamber,[41] and it is difficult to precisely design the acoustic wave profiles using this setup. A potential alternative is to build an array of transducers vibrating at different amplitudes and phases to precisely control an asymmetric acoustic field.[138]

https://doi.org/10.1021/acsnano.2c11680
ACS Nano 2023, 17, 11969−11993

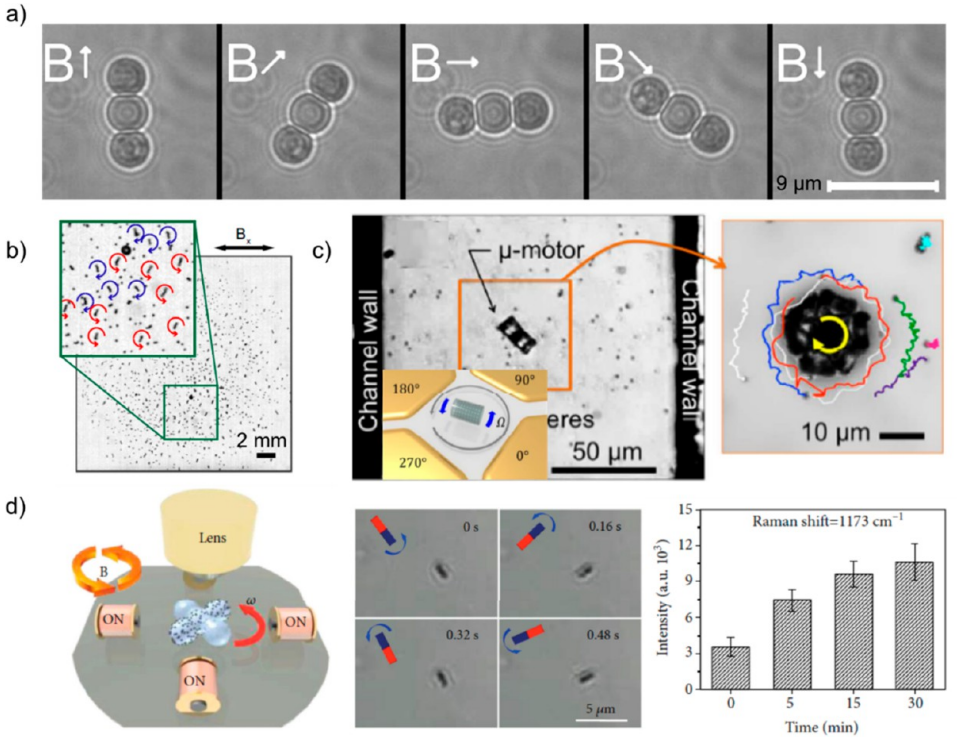

Figure 16. The application of microrotors in micromixing. (a) Rotation of assembled microrotor under rotating magnetic fields. Reproduced with permission under CC BY 3.0 from ref 149. Copyright 2014 IOP Publishing. (b) Snapshot of self-assembled magnetic spinners on a gas−liquid interface. Reproduced with permission under CC BY-NC-ND 4.0 from ref 150. Copyright 2017 National Academy of Sciences USA. (c) A rotating diatom frustule in a microchannel drags passive microparticles by hydrodynamic interaction. Inset: sketch of the rotating electric field setup. Reproduced with permission from ref 151. Copyright 2017 American Chemical Society. (d) Schematic (left) and snapshots (middle) of a rotating "rod-like" microrotor under a rotating magnetic field. (Right) The intensity changes of the prominent peaks of crystal violet being mixed by "rod-like" microrotors. A higher intensity suggests better mixing. Reproduced with permission under CC BY 4.0 from ref 152. Copyright 2020 American Association for the Advancement of Science.

5. APPLICATIONS OF MICROROTORS

The microrotors discussed in the previous sections are becoming increasingly useful in microfluidics and biomedicine and serve as good model systems for soft matter physics. In this section, the research progress of microrotors in microfluidic mixing, biological applications, and their collective behaviors will be briefly reviewed.

5.1. Microfluidic Mixing. Microfluidics has great potential for numerous applications in medicine (e.g., detection of biomarkers, deoxyribonucleic acid (DNA) sequencing, etc.), environmental protection, drug synthesis, etc.[139−144] One major challenge in microfluidic technology is to control mixing at the microscale,[145−147] which originates from the dominant influence of medium viscosity at small scales. Viscosity generally prevents turbulence from occurring in microfluidic devices, which prevents efficient mixing. Microrotors can generate strong vortices, which are an important component of efficient mixing, and thus effectively promotes the mixing of substances in the solution, making them effectively microscopic "stir bars".[148] Furthermore, the interactions among the individual microrotors can lead synergistically to collective phenomena such as active turbulence, making the mixing induced by the ensemble greater than the sum of that of the individual rotors.

Köhler et al.[149] assembled magnetic particles with optical tweezers and then drove them with a rotating magnetic field, attaining photomagnetic powered microrotors that were further applied to a microfluidic channel and generated fluid flows with a speed of 0.4−0.5 μm/s (Figure 16a). Kokot et al.[150] studied the fluid flow at the air−liquid interface induced by the rotation of magnetically driven microspinners. This phenomenon generated "active turbulence", chaotic microflows that exhibited many of the same signatures as turbulent flow (e.g., vorticity, chaos), but at much smaller scales. Because of the efficient mixing associated with turbulence, these microspinners could significantly improve micromixing. At the gas−liquid interface, these magnetic spinners will spontaneously break their symmetries and assemble into chains that can rotate either clockwise or counterclockwise and induce strong vortexes on the interface (Figure 16b). However, it is not clear that these rotors can easily be employed away from the air−liquid interface. Kim et al.[151] integrated the diatom frustule microrotors that rotated over 314 rad/s under rotating electric field. They were used in a microfluidic channel as micromixers. The rotation produced strong flows that advected PS spheres around the microrotor (Figure 16c). Wang et al.[152] chemically synthesized "rod-like" microrotors composed of silica-coated Fe_3O_4 nanoparticles and Ag nanoparticles (Figure 16d, left and middle). These microrotors were applied to surface-enhanced Raman spectroscopy (SERS), where the microrotors significantly enhanced the contact between SERS probe molecules modified on the rod's surface and the analytes, thereby improving the sensitivity of SERS sensing (Figure 16d, right).

5.2. Biological Applications. In the past decade, a substantial body of research has emerged on the use of micro- and nanomotors in biomedicine, such as drug delivery and controllable release, biosensing, disease diagnosis, etc.[8,153−157] In comparison, microrotors confer advantages for biomedical

https://doi.org/10.1021/acsnano.2c11680
ACS Nano 2023, 17, 11969−11993

applications, especially by producing powerful vortices that can substantially speed up the mass transport (e.g., of a drug payload) or increase tissue penetration to reach a disease site.[109−111]

Cheng et al.[15] manipulated an Ni rod to rotate along its *z*-axis by a rotational magnetic field, and they successfully accelerated the transport of tissue plasminogen activator (t-PA) in a polydimethylsiloxane (PDMS) microchannel containing a thrombus model. The rate of thrombus dissolution tripled as a result (Figure 17a). Additionally, when this rod-like motor

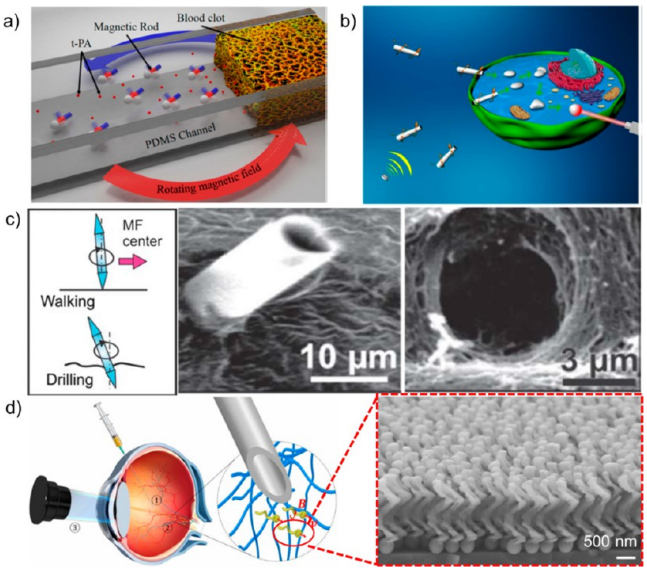

Figure 17. The biological application of microrotors. (a) Sketch of Ni microrods rotating in a microchannel that contains t-PA and thrombus under rotating magnetic field. Reproduced with permission from ref 15. Copyright 2014 American Chemical Society. (b) Schematic of liquid metal gallium microdrillers piercing the cells under ultrasound. Reproduced with permission from ref 158. Copyright 2018 American Chemical Society. (c) (Left) A microdrill with sharp tips. SEM of a microdrill embedded into biological tissue (middle) and a hole (right) after extracting the microdrill. Reproduced with permission under CC BY 3.0 from ref 7. Copyright 2013 Royal Society of Chemistry. (d) Schematic of the helical microdrillers moving in animal's eye (left). SEM of helical microdrillers (right), from ref 16. Copyright The Authors, some rights reserved; exclusive licensee AAAS. Distributed under a CC BY-NC 4.0 license http://creativecommons.org/licenses/by-nc/4.0/. Reprinted with permission from AAAS.

rotated about its long axis under an external field, it acted as a drill and penetrated and moved through the tissues that were more viscous than water. For this reason, these microdrills are promising in minimally invasive surgery, intracellular targeted therapy, and drug delivery in viscoelastic tissues. Taking the microdrill idea further, Xi et al.[7] and Wang et al.[158] successfully inserted a ferromagnetic nanorod with a sharp end and a liquid metal nanorod into a cell through magnetic fields and ultrasound, respectively (Figure 17b,c). In both cases, the nanorod was rotated in a rotating magnetic/acoustic field. Wu et al.[16] further reduced the interaction between a microdrill and the viscous biomolecules in the vitreous of an eyeball by coating the rotor surface with superslippery molecules (Figure 17d).

5.3. Collective Behavior of Microrotors. Collective behaviors of individual organisms are ubiquitous in nature, such as the schooling of fish[159] and the flocking of birds.[160] Similarly, synthetic microswimmers can often self-assemble into complex structures of interesting collective behaviors through hydrodynamic, phoretic, or electromagnetic interactions.[55,161−168] An in-depth study of these phenomena is of great importance for our understanding of nature and for the advancement of biomimetic materials with life-like functionalities. Microrotors can become a useful model for this research. We refer the readers to a recent review article for more uses of microrotors in the study of active matter.[21]

For example, Han et al.[118] assembled ferromagnetic Ni spinners dispersed on the gas−liquid interface into linear chains of approximately equal length using a rotating magnetic field. At higher density of spinners, these chains moved closer to each other, leading to an active spinner lattice that self-heals because of the repulsive hydrodynamic interaction from each spinner (Figure 18a). The resulting active spinner lattice can also transport inert particles by flows. Furthermore, Xie et al.[168] observed various collective behaviors—the formation of vortices, chains, liquids, and ribbons—of peanut-shaped hematite nanoparticles in multimode magnetic fields (Figure 18b). By reversibly switching between these collective formations, the microrobotic swarms can move through narrow channels and synergistically transport large loads, exhibiting high environmental adaptability and the capability to multitask. Microrollers are also known to interact with each other, especially via hydrodynamics, to give rise to interesting patterns and collective behaviors.[169−171] For example, Figure 18c illustrates a chain of paramagnetic microspheres rolling under a rotating magnetic field.[170]

Moving beyond microrotors of simple shapes, Wang et al.[172−174] designed a magnetic microraft was designed with edges shaped like a cosine function. The presence of such curved edges generated additional capillary forces that changed with the arc angle θ at the raft edges, leading to various collective formations.

6. CONCLUSION AND OUTLOOK

We have systematically reviewed the research progress of microrotors in recent years. The key principle of a microrotor is to introduce well-defined torques, and this can be done by breaking chiral symmetry in particle shapes, in the material composition and surface functionalization, or in the way energy is applied. A combination of these three leads to seven distinct types of microrotor designs that we have identified using a three-digit binary index (e.g., "001"). These rotor designs can be powered by chemistry, electromagnetic fields (including light), ultrasound, and roll, spin, or orbit. These microrotors can enhance fluid mixing in microfluidic chips or serve as microdrills for biomedical applications. Their interactions, on the other hand, give rise to interesting collective behaviors that are attractive in the field of active matter.

Looking forward, we see a few challenges and, at the same time, research opportunities for microrotors.

Making Microrotors. At present, the preparation of microrotors is limited to a handful of fabrication methods such as photolithography, GLAD, and electrodeposition. These methods are often complicated, costly, and unsuitable for mass production. A simple, cheap, and controllable method for the synthesis of microrotors in large quantities with good uniformity remains to be found. On this front, our recent report of the chemical synthesis of tadpole-shaped, Ag-containing microrotors shows promise,[24] but much effort is needed to improve its controllability, yield, and sample uniformity.

https://doi.org/10.1021/acsnano.2c11680
ACS Nano 2023, 17, 11969−11993

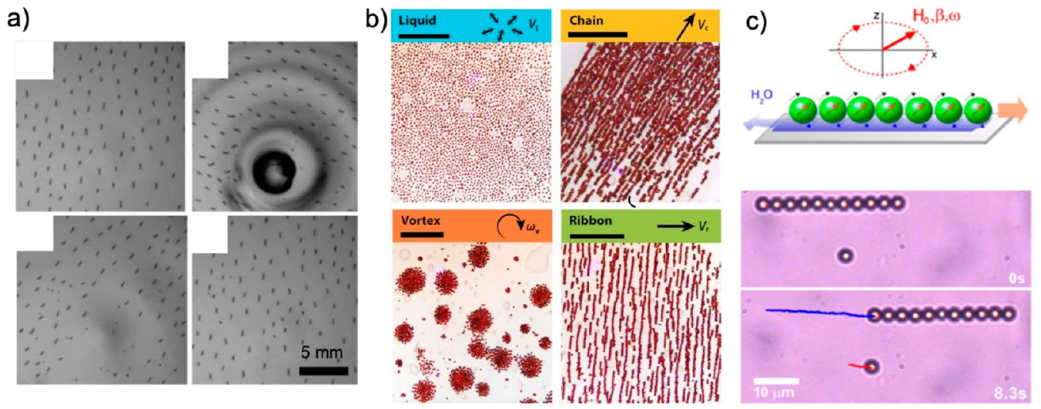

Figure 18. Collective behaviors of microrotors driven by magnetic field. (a) Ferromagnetic Ni spinners spontaneously form active spinner lattice with self-healing behavior on the gas−liquid interface, from ref 118. Copyright The Authors, some rights reserved; exclusive licensee AAAS. Distributed under a CC BY-NC 4.0 license http://creativecommons.org/licenses/by-nc/4.0/. Reprinted with permission from AAAS. (b) Four collective formations (liquid, chain, vortex, ribbon) self-assembled by peanut-shaped particles under a multimode magnetic field. Reproduced with permission from ref 168. Copyright 2019 American Association for the Advancement of Science. (c) A chain of paramagnetic spheres formed under a rotating magnetic field. Reproduced with permission from ref 170. Copyright 2015 American Physical Society.

Chemical Microrotors. The majority of microrotors reported so far that exhibit collective behaviors are powered by electromagnetic fields, which limits the interactions among microrotors to be hydrodynamic or electromagnetic. Nature, on the other hand, takes advantage of chemical signals, and it is tempting to design microrotors that interact in the same way.[175] There are, however, practical limitations. For one, a popular fuel for chemically powered microrotors is H_2O_2, the decomposition of which often produces bubbles in a dense rotor population, which makes observation and quantification difficult. Second, many chemical microrotors are driven by self-generated electric fields[176] (in the form of self-electrophoresis or electrolyte self-diffusiophoresis), which decreases in magnitude in salt solutions.[177−179] Therefore, it is important to develop alternative fuels (such as hydroquinone,[84,97] ethanol,[180,181] and triethylamine[182]) and rotor designs that are insensitive to ionic strength.[183] For example, our recent study[184] has revealed that micromotors and rotors powered by self-electrophoresis are inherently better suited for experiments of high population density because they do not produce net ions.

Biomedical Applications. Current microrotor designs can be improved in a few aspects for better service in biomedical applications. First, microrotors need to be made of biocompatible materials, such as SiO_2 and TiO_2 that are already in use for fabricating microrotors, as well as biodegradable polymers such as poly(lactic-*co*-glycolic acid) (PLGA) and polycaprolactone (PCL).[185] Second, most microrotors can only rotate in a small area, while in reality, rotors may be needed to travel in large distances and in complex environments. For example, spontaneous rotation may be therapeutically useful in certain biomedical scenarios, e.g., enhancing fluid mixing in the bladder[186] or mechanically disrupting a tumor. In these cases, the microrotor may need to travel a nontrivial distance (e.g., through the circulatory or lymphatic system) from its point of administration to the location where it is expected to perform rotation. This challenge could be addressed by developing rotors that are transported passively (or actively translated) to reach the desired location, whereupon their rotational motion is activated. This could be achieved, in principle, by fabricating a rotor−motor complex that can execute different translational or rotational functions at different times (e.g., by applying a different magnetic field waveform). Although there have been a few recent demonstrations,[168,187,188] our capability in this direction is still limited. Finally, with proper surface functionalization and structural design, microrotors can be made into a multifunctional micromachine in the same way as micromotors. They can then perform sophisticated operations such as releasing drugs or retrieving samples while rolling, spinning, or orbiting in a biologically relevant environment.

Controlled Orbiting. Among the three modes of a microrotor, the orbital motion is perhaps the least studied and used, and this could be due to its poor controllability. In fact, a microrotor moving in curved trajectories is often regarded as an imperfect *micromotor*, rather than a *microrotor*. However, orbiting motion is useful in scenarios where the periphery of a sample (such as a cell or a microorganism) needs to be constantly monitored or when a micromachine needs to return to a reporting site after completing a mission. The key in achieving precise control in orbiting requires precise control in both the rotation of the particle and its linear translation, which together determine the radius of the orbit as well as its consistency. Because these two aspects can be decoupled from each other, a microrotor orbiting in an arbitrary radius and at an arbitrary angular speed can, in principle, be precisely designed.

More Ways to Rotate. It is interesting to imagine different ways to break axial-symmetry and introduce torques beyond the 7 strategies that we have discussed throughout this article. As a quick example, the rotation of a Quincke roller, described in section 4.3.3, suggests that torques can spontaneously emerge out of instability even when everything seems to be uniform. Other types of instability could also lead to spontaneous rotation, but we do not know any example. Another possibility is to break symmetry in the physical landscape, such as a Brownian ratchet that rectifies random diffusion into directional motion,[189] or anchoring a colloidal particle to a nematic liquid with a rotating director field.[190,191] Finally, borrowing from the concept of cyborgs and hybrid micromachines,[192−194] we expect many possibilities to arise from the incorporation of biological microrotors, such as bacteria,[195] algae,[196] and embryos,[197] with synthetic ones.

https://doi.org/10.1021/acsnano.2c11680
ACS Nano 2023, 17, 11969−11993

AUTHOR INFORMATION

Corresponding Authors

Wei Wang − *School of Materials Science and Engineering, Harbin Institute of Technology (Shenzhen), Shenzhen, Guangdong 518055, China;* orcid.org/0000-0003-4163-3173; Email: weiwangsz@hit.edu.cn

Jeffrey Lawrence Moran − *Department of Mechanical Engineering, George Mason University, Manassas, Virginia 20110, United States;* orcid.org/0000-0002-0464-0385; Email: jmoran23@gmu.edu

Authors

Xianglong Lyu − *School of Materials Science and Engineering, Harbin Institute of Technology (Shenzhen), Shenzhen, Guangdong 518055, China;* Present Address: X. L., Physical Intelligence Department, Max Planck Institute for Intelligent Systems, Stuttgart 70569, Germany

Jingyuan Chen − *School of Materials Science and Engineering, Harbin Institute of Technology (Shenzhen), Shenzhen, Guangdong 518055, China;* Present Address: J. C., Department of Chemistry, The University of Hong Kong, Hong Kong 999077, China

Ruitong Zhu − *School of Materials Science and Engineering, Harbin Institute of Technology (Shenzhen), Shenzhen, Guangdong 518055, China*

Jiayu Liu − *School of Materials Science and Engineering, Harbin Institute of Technology (Shenzhen), Shenzhen, Guangdong 518055, China*

Lingshan Fu − *School of Materials Science and Engineering, Harbin Institute of Technology (Shenzhen), Shenzhen, Guangdong 518055, China*

Complete contact information is available at: https://pubs.acs.org/10.1021/acsnano.2c11680

Notes

The authors declare no competing financial interest.

ACKNOWLEDGMENTS

W.W. acknowledges the financial support by the Shenzhen Science and Technology Program (RCYX20210609103122038, JCYJ20190806144807401, JCYJ20210324121408022). J.L.M. acknowledges the support of the George Mason University Department of Mechanical Engineering through startup funds. J.L.M. would like to dedicate this article to the memory of Rebecca Hartley (1963-2022).

VOCABULARY

Microrotor: a synthetic object, with at least one dimension smaller than 100 μm, that converts ambient energy into spontaneous rotation (about its own center of mass).

Spinner: a subtype of microrotor that undergoes rotation about its own center of mass without translating significantly.

Orbiter: a subtype of microrotor that travels in a circular "orbital" trajectory, usually from a combination of spinning and translation.

Roller: a subtype of microrotor, similar to an orbiter in that it combines translation and spinning, but instead travels in a straight trajectory along a nearby wall.

Janus particle: a microparticle with two faces pointing in opposite directions (named after the two-faced Roman god of beginnings and endings).

Proximate: closest in relationship; immediate (typically used in reference to a causal relationship).

Chiral: a term used in several branches of physics, referring to a shape or structure that is distinguishable from its mirror image. In this work, we describe diverse ways in which chiral symmetry can be broken, thus inducing a "handedness" to a microrotor and causing it to rotate in a particular direction.

REFERENCES

(1) Luo, M.; Feng, Y.; Wang, T.; Guan, J. Micro-/Nanorobots at Work in Active Drug Delivery. *Adv. Funct. Mater.* **2018**, *28* (25), 1706100.

(2) Choi, J.; Hwang, J.; Kim, J.-y.; Choi, H. Recent Progress in Magnetically Actuated Microrobots for Targeted Delivery of Therapeutic Agents. *Adv. Healthcare Mater.* **2021**, *10* (6), 2001596.

(3) Akolpoglu, M. B.; Alapan, Y.; Dogan, N. O.; Baltaci, S. F.; Yasa, O.; Tural, G. A.; Sitti, M. Magnetically steerable bacterial microrobots moving in 3D biological matrices for stimuli-responsive cargo delivery. *Science Advances* **2022**, *8* (28), eaho6163.

(4) Sridhar, V.; Podjaski, F.; Alapan, Y.; Kroeger, J.; Grunenberg, L.; Kishore, V.; Lotsch, B. V.; Sitti, M. Light-driven carbon nitride microswimmers with propulsion in biological and ionic media and responsive on-demand drug delivery. *Science Robotics* **2022**, *7* (62), eabm1421.

(5) Nelson, B. J.; Kaliakatsos, I. K.; Abbott, J. J. Microrobots for Minimally Invasive Medicine. *Annu. Rev. Biomed. Eng.* **2010**, *12*, 55−85.

(6) Srivastava, S. K.; Medina-Sanchez, M.; Koch, B.; Schmidt, O. G. Medibots: Dual-Action Biogenic Microdaggers for Single-Cell Surgery and Drug Release. *Adv. Mater.* **2016**, *28* (5), 832−837.

(7) Xi, W.; Solovev, A. A.; Ananth, A. N.; Gracias, D. H.; Sanchez, S.; Schmidt, O. G. Rolled-up magnetic microdrillers: towards remotely controlled minimally invasive surgery. *Nanoscale* **2013**, *5* (4), 1294−1297.

(8) Kong, L.; Guan, J.; Pumera, M. Micro- and nanorobots based sensing and biosensing. *Current Opinion in Electrochemistry* **2018**, *10*, 174−182.

(9) Yuan, K.; Bujalance-Fernandez, J.; Jurado-Sanchez, B.; Escarpa, A. Light-driven nanomotors and micromotors: envisioning new analytical possibilities for bio-sensing. *Microchimica Acta* **2020**, *187* (10), 581.

(10) Parmar, J.; Vilela, D.; Villa, K.; Wang, J.; Sanchez, S. Micro- and Nanomotors as Active Environmental Microcleaners and Sensors. *J. Am. Chem. Soc.* **2018**, *140* (30), 9317−9331.

(11) Zhou, Y.; Wang, H.; Ma, Z.; Yang, J. K. W.; Ai, Y. Acoustic Vibration-Induced Actuation of Multiple Microrotors in Microfluidics. *Advanced Materials Technologies* **2020**, *5* (9), 2000323.

(12) Kavcic, B.; Babic, D.; Osterman, N.; Podobnik, B.; Poberaj, I. Magnetically actuated microrotors with individual pumping speed and direction control. *Appl. Phys. Lett.* **2009**, *95* (2), 023504.

(13) Xiao, Y.; Zhang, J.; Fang, B.; Zhao, X.; Hao, N. Acoustics-Actuated Microrobots. *Micromachines* **2022**, *13* (3), 481.

(14) Thampi, S. P.; Doostmohammadi, A.; Shendruk, T. N.; Golestanian, R.; Yeomans, J. M. Active micromachines: Microfluidics powered by mesoscale turbulence. *Science Advances* **2016**, *2* (7), e1501854.

(15) Cheng, R.; Huang, W.; Huang, L.; Yang, B.; Mao, L.; Jin, K.; ZhuGe, Q.; Zhao, Y. Acceleration of Tissue Plasminogen Activator-Mediated Thrombolysis by Magnetically Powered Nanomotors. *ACS Nano* **2014**, *8* (8), 7746−7754.

(16) Wu, Z.; Troll, J.; Jeong, H.-H.; Wei, Q.; Stang, M.; Ziemssen, F.; Wang, Z.; Dong, M.; Schnichels, S.; Qiu, T.; Fischer, P. A swarm of slippery micropropellers penetrates the vitreous body of the eye. *Science Advances* **2018**, *4* (11), eaat4388.

(17) Oppenheimer, N.; Stein, D. B.; Ben Zion, M. Y.; Shelley, M. J. Hyperuniformity and phase enrichment in vortex and rotor assemblies. *Nat. Commun.* **2022**, *13* (1), 804.

(18) Yah Ben Zion, M.; Modin, A.; Chaikin, P. M. Hydrodynamic spin-orbit coupling in asynchronous optically driven micro-rotors. *arXiv* 2203.11051, 2022. https://ui.adsabs.harvard.edu/abs/2022arXiv220311051Y (accessed March 01, 2022).

(19) Huang, Z.-F.; Menzel, A. M.; Loewen, H. Dynamical Crystallites of Active Chiral Particles. *Phys. Rev. Lett.* **2020**, *125* (21), 218002.
(20) Lei, Q.-L.; Ciamarra, M. P.; Ni, R. Nonequilibrium strongly hyperuniform fluids of circle active particles with large local density fluctuations. *Science Advances* **2019**, *5* (1), eaau7423.
(21) Liebchen, B.; Levis, D. Chiral active matter. *Europhys. Lett.* **2022**, *139* (6), 67001.
(22) Qin, L.; Banholzer, M. J.; Xu, X.; Huang, L.; Mirkin, C. A. Rational design and synthesis of catalytically driven nanorotors. *J. Am. Chem. Soc.* **2007**, *129* (48), 14870−14871.
(23) Wang, Y.; Fei, S.-t.; Byun, Y.-M.; Lammert, P. E.; Crespi, V. H.; Sen, A.; Mallouk, T. E. Dynamic Interactions between Fast Microscale Rotors. *J. Am. Chem. Soc.* **2009**, *131* (29), 9926−9927.
(24) Lv, X.; Xiao, Z.; Zhou, C.; Wang, Y.; Duan, S.; Chen, J.; Duan, W.; Ma, X.; Wang, W. Tadpole-Shaped Catalytic Janus Microrotors Enabled by Facile and Controllable Growth of Silver Nanotails. *Adv. Funct. Mater.* **2020**, *30* (46), 2004858.
(25) Fattah, Z.; Loget, G.; Lapeyre, V.; Garrigue, P.; Warakulwit, C.; Limtrakul, J.; Bouffier, L.; Kuhn, A. Straightforward single-step generation of microswimmers by bipolar electrochemistry. *Electrochim. Acta* **2011**, *56* (28), 10562−10566.
(26) Gibbs, J. G.; Sarkar, S.; Holterhoff, A. L.; Li, M.; Castaneda, J.; Toller, J. Engineering the Dynamics of Active Colloids by Targeted Design of Metal-Semiconductor Heterojunctions. *Advanced Materials Interfaces* **2019**, *6* (6), 1801894.
(27) Gibbs, J. G.; Kothari, S.; Saintillan, D.; Zhao, Y. P. Geometrically Designing the Kinematic Behavior of Catalytic Nanomotors. *Nano Lett.* **2011**, *11* (6), 2543−2550.
(28) Gibbs, J. G.; Zhao, Y. Self-Organized Multiconstituent Catalytic Nanomotors. *Small* **2010**, *6* (15), 1656−1662.
(29) Catchmark, J. M.; Subramanian, S.; Sen, A. Directed rotational motion of microscale objects using interfacial tension gradients continually generated via catalytic reactions. *Small* **2005**, *1* (2), 202−206.
(30) Brooks, A. M.; Tasinkevych, M.; Sabrina, S.; Velegol, D.; Sen, A.; Bishop, K. J. M. Shape-directed rotation of homogeneous micromotors via catalytic self-electrophoresis. *Nat. Commun.* **2019**, *10*, 495.
(31) Maggi, C.; Simmchen, J.; Saglimbeni, F.; Katuri, J.; Dipalo, M.; De Angelis, F.; Sanchez, S.; Di Leonardo, R. Self-Assembly of Micromachining Systems Powered by Janus Micromotors. *Small* **2016**, *12* (4), 446−451.
(32) Sokolov, A.; Apodaca, M. M.; Grzybowski, B. A.; Aranson, I. S. Swimming bacteria power microscopic gears. *Proc. Natl. Acad. Sci. U.S.A.* **2010**, *107* (3), 969−974.
(33) Di Leonardo, R.; Angelani, L.; Dell'Arciprete, D.; Ruocco, G.; Iebba, V.; Schippa, S.; Conte, M. P.; Mecarini, F.; De Angelis, F.; Di Fabrizio, E. Bacterial ratchet motors. *Proc. Natl. Acad. Sci. U.S.A.* **2010**, *107* (21), 9541−9545.
(34) Kuemmel, F.; ten Hagen, B.; Wittkowski, R.; Buttinoni, I.; Eichhorn, R.; Volpe, G.; Loewen, H.; Bechinger, C. Circular Motion of Asymmetric Self-Propelling Particles. *Phys. Rev. Lett.* **2013**, *110* (19), 198302.
(35) Liu, M.; Zentgraf, T.; Liu, Y.; Bartal, G.; Zhang, X. Light-driven nanoscale plasmonic motors. *Nat. Nanotechnol.* **2010**, *5* (8), 570−573.
(36) Tierno, P.; Golestanian, R.; Pagonabarraga, I.; Sagues, F. Magnetically Actuated Colloidal Microswimmers. *J. Phys. Chem. B* **2008**, *112* (51), 16525−16528.
(37) Tierno, P.; Golestanian, R.; Pagonabarraga, I.; Sagues, F. Controlled Swimming in Confined Fluids of Magnetically Actuated Colloidal Rotors. *Phys. Rev. Lett.* **2008**, *101* (21), 218304.
(38) Wang, Z.; Wang, Z.; Li, J.; Cheung, S. T. H.; Tian, C.; Kim, S.-H.; Yi, G.-R.; Ducrot, E.; Wang, Y. Active Patchy Colloids with Shape-Tunable Dynamics. *J. Am. Chem. Soc.* **2019**, *141* (37), 14853−14863.
(39) Kim, K.; Guo, J.; Xu, X.; Fan, D. Micromotors with Step-Motor Characteristics by Controlled Magnetic Interactions among Assembled Components. *ACS Nano* **2015**, *9* (1), 548−554.
(40) Fan, D. L.; Zhu, F. Q.; Xu, X.; Cammarata, R. C.; Chien, C. L. Electronic properties of nanoentities revealed by electrically driven rotation. *Proc. Natl. Acad. Sci. U.S.A.* **2012**, *109* (24), 9309−9313.
(41) Zhou, C.; Zhao, L.; Wei, M.; Wang, W. Twists and Turns of Orbiting and Spinning Metallic Microparticles Powered by Megahertz Ultrasound. *ACS Nano* **2017**, *11* (12), 12668−12676.
(42) Wang, W.; Castro, L. A.; Hoyos, M.; Mallouk, T. E. Autonomous Motion of Metallic Microrods Propelled by Ultrasound. *ACS Nano* **2012**, *6* (7), 6122−6132.
(43) Ahmed, S.; Wang, W.; Bai, L.; Gentekos, D. T.; Hoyos, M.; Mallouk, T. E. Density and Shape Effects in the Acoustic Propulsion of Bimetallic Nanorod Motors. *ACS Nano* **2016**, *10* (4), 4763−4769.
(44) Alapan, Y.; Yigit, B.; Beker, O.; Demirors, A. F.; Sitti, M. Shape-encoded dynamic assembly of mobile micromachines. *Nat. Mater.* **2019**, *18* (11), 1244−1251.
(45) Archer, R. J.; Campbell, A. I.; Ebbens, S. J. Glancing angle metal evaporation synthesis of catalytic swimming Janus colloids with well defined angular velocity. *Soft Matter* **2015**, *11* (34), 6872−6880.
(46) Sabrina, S.; Tasinkevych, M.; Ahmed, S.; Brooks, A. M.; Olvera de la Cruz, M.; Mallouk, T. E.; Bishop, K. J. M. Shape-Directed Microspinners Powered by Ultrasound. *ACS Nano* **2018**, *12* (3), 2939−2947.
(47) Andren, D.; Baranov, D. G.; Jones, S.; Volpe, G.; Verre, R.; Kall, M. Microscopic metavehicles powered and steered by embedded optical metasurfaces. *Nat. Nanotechnol.* **2021**, *16* (9), 970−974.
(48) Wu, X.; Ehehalt, R.; Razinskas, G.; Feichtner, T.; Qin, J.; Hecht, B. Light-driven microdrones. *Nat. Nanotechnol.* **2022**, *17* (5), 477−484.
(49) Aubret, A.; Youssef, M.; Sacanna, S.; Palacci, J. Targeted assembly and synchronization of self-spinning microgears. *Nat. Phys.* **2018**, *14* (11), 1114−1118.
(50) Aubret, A.; Palacci, J. Diffusiophoretic design of self-spinning microgears from colloidal microswimmers. *Soft Matter* **2018**, *14* (47), 9577−9588.
(51) Davies Wykes, M. S.; Palacci, J.; Adachi, T.; Ristroph, L.; Zhong, X.; Ward, M. D.; Zhang, J.; Shelley, M. J. Dynamic self-assembly of microscale rotors and swimmers. *Soft Matter* **2016**, *12* (20), 4584−4589.
(52) Ebbens, S.; Jones, R. A. L.; Ryan, A. J.; Golestanian, R.; Howse, J. R. Self-assembled autonomous runners and tumblers. *Phys. Rev. E* **2010**, *82* (1), 015304.
(53) Lv, X.; Du, S.; Zhou, C.; Wang, W.; Wang, H.; Zhang, Z. Synthesis of Snowman-shaped Photocatalytic Microrotors and Mechanical Micropumps. *Chemnanomat* **2021**, *7* (8), 902−905.
(54) Mair, L. O.; Evans, B. A.; Nacev, A.; Stepanov, P. Y.; Hilaman, R.; Chowdhury, S.; Jafari, S.; Wang, W.; Shapiro, B.; Weinberg, I. N. Magnetic microkayaks: propulsion of microrods precessing near a surface by kilohertz frequency, rotating magnetic fields. *Nanoscale* **2017**, *9* (10), 3375−3381.
(55) Yan, J.; Bloom, M.; Bae, S. C.; Luijten, E.; Granick, S. Linking synchronization to self-assembly using magnetic Janus colloids. *Nature* **2012**, *491* (7425), 578−581.
(56) Tottori, S.; Zhang, L.; Qiu, F.; Krawczyk, K. K.; Franco-Obregon, A.; Nelson, B. J. Magnetic Helical Micromachines: Fabrication, Controlled Swimming, and Cargo Transport. *Adv. Mater.* **2012**, *24* (6), 811−816.
(57) Ghosh, A.; Fischer, P. Controlled Propulsion of Artificial Magnetic Nanostructured Propellers. *Nano Lett.* **2009**, *9* (6), 2243−2245.
(58) Kim, M.; Powers, T. R. Hydrodynamic interactions between rotating helices. *Phys. Rev. E* **2004**, *69* (6), 061910.
(59) Reichert, M.; Stark, H. Synchronization of rotating helices by hydrodynamic interactions. *Eur. Phys. J. E* **2005**, *17* (4), 493−500.
(60) Jones, P. H.; Palmisano, F.; Bonaccorso, F.; Gucciardi, P. G.; Calogero, G.; Ferrari, A. C.; Marago, O. M. Rotation Detection in Light-Driven Nanorotors. *ACS Nano* **2009**, *3* (10), 3077−3084.
(61) Yan, Z.; Scherer, N. F. Optical Vortex Induced Rotation of Silver Nanowires. *J. Phys. Chem. Lett.* **2013**, *4* (17), 2937−2942.
(62) Lehmuskero, A.; Ogier, R.; Gschneidtner, T.; Johansson, P.; Kall, M. Ultrafast Spinning of Gold Nanoparticles in Water Using Circularly Polarized Light. *Nano Lett.* **2013**, *13* (7), 3129−3134.
(63) Zhang, S.; Elsayed, M.; Peng, R.; Chen, Y.; Zhang, Y.; Peng, J.; Li, W.; Chamberlain, M. D.; Nikitina, A.; Yu, S.; Liu, X.; Neale, S. L.;

https://doi.org/10.1021/acsnano.2c11680
ACS Nano 2023, 17, 11969−11993

Wheeler, A. R. Reconfigurable multi-component micromachines driven by optoelectronic tweezers. *Nat. Commun.* **2021**, *12* (1), 5349.
(64) Ding, H.; Kollipara, P. S.; Kim, Y.; Kotnala, A.; Li, J.; Chen, Z.; Zheng, Y. Universal optothermal micro/nanoscale rotors. *Science Advances* **2022**, *8* (24), eabn8498.
(65) Xu, X.; Liu, C.; Kim, K.; Fan, D. L. Electric-Driven Rotation of Silicon Nanowires and Silicon Nanowire Motors. *Adv. Funct. Mater.* **2014**, *24* (30), 4843−4850.
(66) Kim, K.; Xu, X.; Guo, J.; Fan, D. L. Ultrahigh-speed rotating nanoelectromechanical system devices assembled from nanoscale building blocks. *Nat. Commun.* **2014**, *5*, 3632.
(67) Du, S.; Wang, H.; Zhou, C.; Wang, W.; Zhang, Z. Motor and Rotor in One: Light-Active ZnO/Au Twinned Rods of Tunable Motion Modes. *J. Am. Chem. Soc.* **2020**, *142* (5), 2213−2217.
(68) Zhang, L.; Petit, T.; Lu, Y.; Kratochvil, B. E.; Peyer, K. E.; Pei, R.; Lou, J.; Nelson, B. J. Controlled Propulsion and Cargo Transport of Rotating Nickel Nanowires near a Patterned Solid Surface. *ACS Nano* **2010**, *4* (10), 6228−6234.
(69) Garcia-Torres, J.; Calero, C.; Sagues, F.; Pagonabarraga, I.; Tierno, P. Magnetically tunable bidirectional locomotion of a self-assembled nanorod-sphere propeller. *Nat. Commun.* **2018**, *9*, 1663.
(70) Yang, T.; Tomaka, A.; Tasci, T. O.; Neeves, K. B.; Wu, N.; Marr, D. W. M. Microwheels on microroads: Enhanced translation on topographic surfaces. *Science Robotics* **2019**, *4* (32), eaaw9525.
(71) Marine, N. A.; Wheat, P. M.; Ault, J.; Posner, J. D. Diffusive behaviors of circle-swimming motors. *Phys. Rev. E* **2013**, *87* (5), 052305.
(72) Mano, N.; Heller, A. Bioelectrochemical propulsion. *J. Am. Chem. Soc.* **2005**, *127* (33), 11574−11575.
(73) Gao, W.; Pei, A.; Feng, X.; Hennessy, C.; Wang, J. Organized Self-Assembly of Janus Micromotors with Hydrophobic Hemispheres. *J. Am. Chem. Soc.* **2013**, *135* (3), 998−1001.
(74) Wang, D.; Jiang, J.; Hao, B.; Li, M.; Chen, Z.; Zhang, H.; Wang, X.; Dong, B. Bio-inspired micro/nanomotor with visible light dependent in situ rotation and phototaxis. *Appl. Mater. Today* **2022**, *29*, 101652.
(75) Mano, T.; Delfau, J.-B.; Iwasawa, J.; Sano, M. Optimal run-and-tumble−based transportation of a Janus particle with active steering. *Proc. Natl. Acad. Sci. U. S. A.* **2017**, *114* (13), E2580−E2589.
(76) Boymelgreen, A.; Yossifon, G.; Park, S.; Miloh, T. Spinning Janus doublets driven in uniform ac electric fields. *Phys. Rev. E* **2014**, *89* (1), 011003.
(77) Liu, R.; Sen, A. Autonomous Nanomotor Based on Copper-Platinum Segmented Nanobattery. *J. Am. Chem. Soc.* **2011**, *133* (50), 20064−20067.
(78) Zhang, H.; Koens, L.; Lauga, E.; Mourran, A.; Moeller, M. A Light-Driven Microgel Rotor. *Small* **2019**, *15* (46), 1903379.
(79) Shields, C. W.; Han, K.; Ma, F.; Miloh, T.; Yossifon, G.; Velev, O. D. Supercolloidal Spinners: Complex Active Particles for Electrically Powered and Switchable Rotation. *Adv. Funct. Mater.* **2018**, *28* (35), 1803465.
(80) Nadal, F.; Lauga, E. Asymmetric steady streaming as a mechanism for acoustic propulsion of rigid bodies. *Phys. Fluids* **2014**, *26* (8), 082001.
(81) Kaynak, M.; Ozcelik, A.; Nourhani, A.; Lammert, P. E.; Crespi, V. H.; Huang, T. J. Acoustic actuation of bioinspired microswimmers. *Lab Chip* **2017**, *17* (3), 395−400.
(82) Ahmed, D.; Lu, M.; Nourhani, A.; Lammert, P. E.; Stratton, Z.; Muddana, H. S.; Crespi, V. H.; Huang, T. J. Selectively manipulable acoustic-powered microswimmers. *Sci. Rep.* **2015**, *5*, 9744.
(83) Venkateshwar Rao, D.; Reddy, N.; Fransaer, J.; Clasen, C. Self-propulsion of bent bimetallic Janus rods. *J. Phys. D: Appl. Phys.* **2019**, *52* (1), 014002.
(84) Wang, J.; Xiong, Z.; Zhan, X.; Dai, B.; Zheng, J.; Liu, J.; Tang, J. A Silicon Nanowire as a Spectrally Tunable Light-Driven Nanomotor. *Adv. Mater.* **2017**, *29* (30), 1701451.
(85) He, Y.; Wu, J.; Zhao, Y. Designing catalytic nanomotors by dynamic shadowing growth. *Nano Lett.* **2007**, *7* (5), 1369−1375.
(86) Zheng, J.; Wang, J.; Xiong, Z.; Wan, Z.; Zhan, X.; Yang, S.; Chen, J.; Dai, J.; Tang, J. Full Spectrum Tunable Visible-Light-Driven Alloy Nanomotor. *Adv. Funct. Mater.* **2019**, *29* (27), 1901768.
(87) Zhang, X.; Xie, W.; Wang, H.; Zhang, Z. Magnetic matchstick micromotors with switchable motion modes. *Chem. Commun.* **2021**, *57* (31), 3797−3800.
(88) Maggi, C.; Saglimbeni, F.; Dipalo, M.; De Angelis, F.; Di Leonardo, R. Micromotors with asymmetric shape that efficiently convert light into work by thermocapillary effects. *Nat. Commun.* **2015**, *6*, 7855.
(89) Ni, S.; Marini, E.; Buttinoni, I.; Wolf, H.; Isa, L. Hybrid colloidal microswimmers through sequential capillary assembly. *Soft Matter* **2017**, *13* (23), 4252−4259.
(90) Zhang, J.; Granick, S. Natural selection in the colloid world: active chiral spirals. *Faraday Discuss.* **2016**, *191*, 35−46.
(91) Ma, F.; Wang, S.; Wu, D. T.; Wu, N. Electric-field-induced assembly and propulsion of chiral colloidal clusters. *Proc. Natl. Acad. Sci. U.S.A.* **2015**, *112* (20), 6307−6312.
(92) Wang, Y.; Hernandez, R. M.; Bartlett, D. J., Jr.; Bingham, J. M.; Kline, T. R.; Sen, A.; Mallouk, T. E. Bipolar electrochemical mechanism for the propulsion of catalytic nanomotors in hydrogen peroxide solutions. *Langmuir* **2006**, *22* (25), 10451−10456.
(93) Zhou, C.; Zhang, H. P.; Tang, J.; Wang, W. Photochemically Powered AgCl Janus Micromotors as a Model System to Understand Ionic Self-Diffusiophoresis. *Langmuir* **2018**, *34* (10), 3289−3295.
(94) Liang, X.; Mou, F.; Huang, Z.; Zhang, J.; You, M.; Xu, L.; Luo, M.; Guan, J. Hierarchical Microswarms with Leader-Follower-Like Structures: Electrohydrodynamic Self-Organization and Multimode Collective Photoresponses. *Adv. Funct. Mater.* **2020**, *30* (16), 1908602.
(95) Yang, M.; Ripoll, M.; Chen, K. Catalytic microrotor driven by geometrical asymmetry. *J. Chem. Phys.* **2015**, *142* (5), 054902.
(96) Wang, J.; Xiong, Z.; Zheng, J.; Zhan, X.; Tang, J. Light-Driven Micro/Nanomotor for Promising Biomedical Tools: Principle, Challenge, and Prospect. *Acc. Chem. Res.* **2018**, *51* (9), 1957−1965.
(97) Zheng, J.; Dai, B.; Wang, J.; Xiong, Z.; Yang, Y.; Liu, J.; Zhan, X.; Wan, Z.; Tang, J. Orthogonal navigation of multiple visible-light-driven artificial microswimmers. *Nat. Commun.* **2017**, *8*, 1438.
(98) Zhan, X.; Zheng, J.; Zhao, Y.; Zhu, B.; Cheng, R.; Wang, J.; Liu, J.; Tang, J.; Tang, J. From Strong Dichroic Nanomotor to Polarotactic Microswimmer. *Adv. Mater.* **2019**, *31* (48), 1903329.
(99) Chen, X.; Xu, Y.; Lou, K.; Peng, Y.; Zhou, C.; Wang, W.; Zhang, H. P. Programmable, Spatiotemporal Control of Colloidal Motion Waves via Structured Light. *ACS Nano* **2022**, *16* (8), 12755−12766.
(100) Beth, R. A. Mechanical detection and measurement of the angular momentum of light. *Phys. Rev.* **1936**, *50* (2), 115−125.
(101) Zong, Y.; Liu, J.; Liu, R.; Guo, H.; Yang, M.; Li, Z.; Chen, K. An Optically Driven Bistable Janus Rotor with Patterned Metal Coatings. *ACS Nano* **2015**, *9* (11), 10844−10851.
(102) Lin, X.-F.; Hu, G.-Q.; Chen, Q.-D.; Niu, L.-G.; Li, Q.-S.; Ostendorf, A.; Sun, H.-B. A light-driven turbine-like micro-rotor and study on its light-to-mechanical power conversion efficiency. *Appl. Phys. Lett.* **2012**, *101* (11), 113901.
(103) Palagi, S.; Mark, A. G.; Reigh, S. Y.; Melde, K.; Qiu, T.; Zeng, H.; Parmeggiani, C.; Martella, D.; Sanchez-Castillo, A.; Kapernaum, N.; Giesselmann, F.; Wiersma, D. S.; Lauga, E.; Fischer, P. Structured light enables biomimetic swimming and versatile locomotion of photo-responsive soft microrobots. *Nat. Mater.* **2016**, *15* (6), 647−653.
(104) Kim, H.; Sundaram, S.; Kang, J.-H.; Tanjeem, N.; Emrick, T.; Hayward, R. C. Coupled oscillation and spinning of photothermal particles in Marangoni optical traps. *Proc. Natl. Acad. Sci. U.S.A.* **2021**, *118* (18), e2024581118.
(105) Nagelberg, S.; Totz, J. F.; Mittasch, M.; Sresht, V.; Zeininger, L.; Swager, T. M.; Kreysing, M.; Kolle, M. Actuation of Janus Emulsion Droplets via Optothermally Induced Marangoni Forces. *Phys. Rev. Lett.* **2021**, *127* (14), 144503.
(106) Bozuyuk, U.; Suadiye, E.; Aghakhani, A.; Dogan, N. O.; Lazovic, J.; Tiryaki, M. E.; Schneider, M.; Karacakol, A. C.; Demir, S. O.; Richter, G.; Sitti, M. High-Performance Magnetic FePt (L1(0)) Surface

https://doi.org/10.1021/acsnano.2c11680
ACS Nano 2023, 17, 11969−11993

Microrollers Towards Medical Imaging-Guided Endovascular Delivery Applications. *Adv. Funct. Mater.* **2022**, *32* (8), 2109741.
(107) Zhou, H.; Mayorga-Martinez, C. C.; Pane, S.; Zhang, L.; Pumera, M. Magnetically Driven Micro and Nanorobots. *Chem. Rev.* **2021**, *121* (8), 4999−5041.
(108) Dong, Y.; Wang, L.; Iacovacci, V.; Wang, X.; Zhang, L.; Nelson, B. J. Magnetic helical micro-/nanomachines: Recent progress and perspective. *Matter* **2022**, *5* (1), 77−109.
(109) Schamel, D.; Mark, A. G.; Gibbs, J. G.; Miksch, C.; Morozov, K. I.; Leshansky, A. M.; Fischer, P. Nanopropellers and their actuation in complex viscoelastic media. *ACS Nano* **2014**, *8* (9), 8794−8801.
(110) Walker, D.; Käsdorf, B. T.; Jeong, H.-H.; Lieleg, O.; Fischer, P. Enzymatically active biomimetic micropropellers for the penetration of mucin gels. *Science Advances* **2015**, *1* (11), e1500501.
(111) Wu, Z.; Troll, J.; Jeong, H.-H.; Wei, Q.; Stang, M.; Ziemssen, F.; Wang, Z.; Dong, M.; Schnichels, S.; Qiu, T. A swarm of slippery micropropellers penetrates the vitreous body of the eye. *Science Advances* **2018**, *4* (11), eaat4388.
(112) Hu, N.; Wang, L.; Zhai, W.; Sun, M.; Xie, H.; Wu, Z.; He, Q. Magnetically Actuated Rolling of Star-Shaped Hydrogel Microswimmer. *Macromol. Chem. Phys.* **2018**, *219* (5), 1700540.
(113) Bozuyuk, U.; Alapan, Y.; Aghakhani, A.; Yunusa, M.; Sitti, M. Shape anisotropy-governed locomotion of surface microrollers on vessel-like microtopographies against physiological flows. *Proc. Natl. Acad. Sci. U.S.A.* **2021**, *118* (13), e2022090118.
(114) Li, T.; Zhang, A.; Shao, G.; Wei, M.; Guo, B.; Zhang, G.; Li, L.; Wang, W. Janus Microdimer Surface Walkers Propelled by Oscillating Magnetic Fields. *Adv. Funct. Mater.* **2018**, *28* (25), 1706066.
(115) Yu, S.; Li, T.; Ji, F.; Zhao, S.; Liu, K.; Zhang, Z.; Zhang, W.; Mei, Y. Trimer-like microrobots with multimodal locomotion and reconfigurable capabilities. *Materials Today Advances* **2022**, *14*, 100231.
(116) Massana-Cid, H.; Levis, D.; Hernández, R. J. H.; Pagonabarraga, I.; Tierno, P. Arrested phase separation in chiral fluids of colloidal spinners. *Physical Review Research* **2021**, *3* (4), L042021.
(117) Soni, V.; Bililign, E. S.; Magkiriadou, S.; Sacanna, S.; Bartolo, D.; Shelley, M. J.; Irvine, W. T. The odd free surface flows of a colloidal chiral fluid. *Nat. Phys.* **2019**, *15* (11), 1188−1194.
(118) Han, K.; Kokot, G.; Das, S.; Winkler, R. G.; Gompper, G.; Snezhko, A. Reconfigurable structure and tunable transport in synchronized active spinner materials. *Science Advances* **2020**, *6* (12), eaaz8535.
(119) Morgan, H.; Green, N. G. *AC electrokinetics: colloids and nanoparticles*; Research Studies Press: Philadelphia, 2002.
(120) Mano, T.; Delfau, J.-B.; Iwasawa, J.; Sano, M. Optimal run-and-tumble-based transportation of a Janus particle with active steering. *Proc. Natl. Acad. Sci. U.S.A.* **2017**, *114* (13), E1936−E1936.
(121) Mano, T.; Delfau, J.-B.; Iwasawa, J.; Sano, M. Optimal run-and-tumble-based transportation of a Janus particle with active steering. *Proc. Natl. Acad. Sci. U.S.A.* **2017**, *114* (13), E2580−E2589.
(122) Pradillo, G. E.; Karani, H.; Vlahovska, P. M. Quincke rotor dynamics in confinement: rolling and hovering. *Soft Matter* **2019**, *15* (32), 6564−6570.
(123) Bricard, A.; Caussin, J.-B.; Das, D.; Savoie, C.; Chikkadi, V.; Shitara, K.; Chepizhko, O.; Peruani, F.; Saintillan, D.; Bartolo, D. Emergent vortices in populations of colloidal rollers. *Nat. Commun.* **2015**, *6*, 7470.
(124) Zhang, Z.; Yuan, H.; Dou, Y.; de la Cruz, M. O.; Bishop, K. J. M. Quincke Oscillations of Colloids at Planar Electrodes. *Phys. Rev. Lett.* **2021**, *126* (25), 258001.
(125) Bricard, A.; Caussin, J.-B.; Desreumaux, N.; Dauchot, O.; Bartolo, D. Emergence of macroscopic directed motion in populations of motile colloids. *Nature* **2013**, *503* (7474), 95−98.
(126) Brosseau, Q.; Hickey, G.; Vlahovska, P. M. Electrohydrodynamic Quincke rotation of a prolate ellipsoid. *Physical Review Fluids* **2017**, *2* (1), 014101.
(127) Vlahovska, P. M. Electrohydrodynamic instabilities of viscous drops. *Physical Review Fluids* **2016**, *1* (6), 060504.
(128) Zhu, L.; Stone, H. A. Propulsion driven by self-oscillation via an electrohydrodynamic instability. *Physical Review Fluids* **2019**, *4* (6), 061701.
(129) Zhang, B.; Snezhko, A.; Sokolov, A. Guiding Self-Assembly of Active Colloids by Temporal Modulation of Activity. *Phys. Rev. Lett.* **2022**, *128* (1), 018004.
(130) Liu, Z. T.; Shi, Y.; Zhao, Y.; Chate, H.; Shi, X.-q.; Zhang, T. H. Activity waves and freestanding vortices in populations of subcritical Quincke rollers. *Proc. Natl. Acad. Sci. U.S.A.* **2021**, *118* (40), e2104724118.
(131) Morin, A.; Bartolo, D. Flowing Active Liquids in a Pipe: Hysteretic Response of Polar Flocks to External Fields. *Physical Review X* **2018**, *8* (2), 021037.
(132) Aziz, A.; Pane, S.; Iacovacci, V.; Koukourakis, N.; Czarske, J.; Menciassi, A.; Medina-Sanchez, M.; Schmidt, O. G. Medical Imaging of Microrobots: Toward In Vivo Applications. *ACS Nano* **2020**, *14* (9), 10865−10893.
(133) Gao, C.; Wang, Y.; Ye, Z.; Lin, Z.; Ma, X.; He, Q. Biomedical Micro-/Nanomotors: From Overcoming Biological Barriers to In Vivo Imaging. *Adv. Mater.* **2021**, *33* (6), 2000512.
(134) Zhou, M.; Gao, D.; Yang, Z.; Zhou, C.; Tan, Y.; Wang, W.; Jiang, Y. Streaming-enhanced, chip-based biosensor with acoustically active, biomarker-functionalized micropillars: A case study of thrombin detection. *Talanta* **2021**, *222*, 121480.
(135) McNeill, J. M.; Choi, Y. C.; Cai, Y.-Y.; Guo, J.; Nadal, F.; Kagan, C. R.; Mallouk, T. E. Three-Dimensionally Complex Phase Behavior and Collective Phenomena in Mixtures of Acoustically Powered Chiral Microspinners. *ACS Nano* **2023**, *17*, 7911.
(136) Kaynak, M.; Ozcelik, A.; Nama, N.; Nourhani, A.; Lammert, P. E.; Crespi, V. H.; Huang, T. J. Acoustofluidic actuation of in situ fabricated microrotors. *Lab Chip* **2016**, *16* (18), 3532−3537.
(137) Ren, L.; Nama, N.; McNeill, J. M.; Soto, F.; Yan, Z.; Liu, W.; Wang, W.; Wang, J.; Mallouk, T. E. 3D steerable, acoustically powered microswimmers for single-particle manipulation. *Science Advances* **2019**, *5* (10), eaax3084.
(138) Melde, K.; Mark, A. G.; Qiu, T.; Fischer, P. Holograms for acoustics. *Nature* **2016**, *537* (7621), 518−522.
(139) Warren, A. D.; Kwong, G. A.; Wood, D. K.; Lin, K. Y.; Bhatia, S. N. Point-of-care diagnostics for noncommunicable diseases using synthetic urinary biomarkers and paper microfluidics. *Proc. Natl. Acad. Sci. U.S.A.* **2014**, *111* (10), 3671−3676.
(140) Cheng, H.-L.; Fu, C.-Y.; Kuo, W.-C.; Chen, Y.-W.; Chen, Y.-S.; Lee, Y.-M.; Li, K.-H.; Chen, C.; Ma, H.-P.; Huang, P.-C.; Wang, Y.-L.; Lee, G.-B. Detecting miRNA biomarkers from extracellular vesicles for cardiovascular disease with a microfluidic system. *Lab Chip* **2018**, *18* (19), 2917.
(141) Hu, B.; Li, J.; Mou, L.; Liu, Y.; Deng, J.; Qian, W.; Sun, J.; Cha, R.; Jiang, X. An automated and portable microfluidic chemiluminescence immunoassay for quantitative detection of biomarkers. *Lab Chip* **2017**, *17* (13), 2225−2234.
(142) Ruan, Q.; Ruan, W.; Lin, X.; Wang, Y.; Zou, F.; Zhou, L.; Zhu, Z.; Yang, C. Digital-WGS: Automated, highly efficient whole-genome sequencing of single cells by digital microfluidics. *Science Advances* **2020**, *6* (50), eabd6454.
(143) Ding, Y.; Howes, P. D.; deMello, A. J. Recent Advances in Droplet Microfluidics. *Anal. Chem.* **2020**, *92* (1), 132−149.
(144) Liu, Y.; Sun, L.; Zhang, H.; Shang, L.; Zhao, Y. Microfluidics for Drug Development: From Synthesis to Evaluation. *Chem. Rev.* **2021**, *121* (13), 7468−7529.
(145) Shanko, E.-S.; van de Burgt, Y.; Anderson, P. D.; den Toonder, J. M. J. Microfluidic Magnetic Mixing at Low Reynolds Numbers and in Stagnant Fluids. *Micromachines* **2019**, *10* (11), 731.
(146) Stremler, M. A.; Haselton, F. R.; Aref, H. Designing for chaos: applications of chaotic advection at the microscale. *Philosophical Transactions of the Royal Society a-Mathematical Physical and Engineering Sciences* **2004**, *362* (1818), 1019−1036.
(147) Ward, K.; Fan, Z. H. Mixing in microfluidic devices and enhancement methods. *Journal of Micromechanics and Microengineering* **2015**, *25* (9), 094001.

https://doi.org/10.1021/acsnano.2c11680
ACS Nano 2023, 17, 11969−11993

(148) Tallapragada, P.; Sudarsanam, S. Chaotic advection and mixing by a pair of microrotors in a circular domain. *Phys. Rev. E* **2019**, *100* (6), 062207.
(149) Koehler, J.; Ghadiri, R.; Ksouri, S. I.; Guo, Q.; Gurevich, E. L.; Ostendorf, A. Generation of microfluidic flow using an optically assembled and magnetically driven microrotor. *J. Phys. D: Appl. Phys.* **2014**, *47* (50), 505501.
(150) Kokot, G.; Das, S.; Winkler, R. G.; Gompper, G.; Aranson, I. S.; Snezhko, A. Active turbulence in a gas of self-assembled spinners. *Proc. Natl. Acad. Sci. U.S.A.* **2017**, *114* (49), 12870−12875.
(151) Kim, K.; Liang, Z.; Liu, M.; Fan, D. E. Biobased High-Performance Rotary Micromotors for Individually Reconfigurable Micromachine Arrays and Microfluidic Applications. *ACS Appl. Mater. Interfaces* **2017**, *9* (7), 6144−6152.
(152) Wang, Y.; Liu, Y.; Li, Y.; Xu, D.; Pan, X.; Chen, Y.; Zhou, D.; Wang, B.; Feng, H.; Ma, X. Magnetic Nanomotor-Based Maneuverable SERS Probe. *Research* **2020**, *2020* (Unsp), 7962024.
(153) Tu, Y.; Peng, F.; Andre, A. A. M.; Men, Y.; Srinivas, M.; Wilson, D. A. Biodegradable Hybrid Stomatocyte Nanomotors for Drug Delivery. *ACS Nano* **2017**, *11* (2), 1957−1963.
(154) Lin, R.; Yu, W.; Chen, X.; Gao, H. Self-Propelled Micro/Nanomotors for Tumor Targeting Delivery and Therapy. *Adv. Healthcare Mater.* **2021**, *10* (1), 2001212.
(155) Chen, Y.; Pan, R.; Wang, Y.; Guo, P.; Liu, X.; Ji, F.; Hu, J.; Yan, X.; Wang, G. P.; Zhang, L.; Sun, Y.; Ma, X. Carbon Helical Nanorobots Capable of Cell Membrane Penetration for Single Cell Targeted SERS Bio-Sensing and Photothermal Cancer Therapy. *Adv. Funct. Mater.* **2022**, *32* (30), 2200600.
(156) Ye, H.; Wang, Y.; Xu, D.; Liu, X.; Liu, S.; Ma, X. Design and fabrication of micro/nano-motors for environmental and sensing applications. *Appl. Mater. Today* **2021**, *23*, 101007.
(157) Rastmanesh, A.; Tavakkoli Yaraki, M.; Wu, J.; Wang, Z.; Ghoderao, P.; Gao, Y.; Tan, Y. N. Bioinspired micro/nanomotors towards a self-propelled noninvasive diagnosis and treatment of cancer. *Molecular Systems Design & Engineering* **2021**, *6* (8), 566−593.
(158) Wang, D.; Gao, C.; Wang, W.; Sun, M.; Guo, B.; Xie, H.; He, Q. Shape-Transformable, Fusible Rodlike Swimming Liquid Metal Nanomachine. *ACS Nano* **2018**, *12* (10), 10212−10220.
(159) Lopez, U.; Gautrais, J.; Couzin, I. D.; Theraulaz, G. From behavioural analyses to models of collective motion in fish schools. *Interface focus* **2012**, *2* (6), 693−707.
(160) Ballerini, M.; Cabibbo, N.; Candelier, R.; Cavagna, A.; Cisbani, E.; Giardina, I.; Lecomte, V.; Orlandi, A.; Parisi, G.; Procaccini, A.; Viale, M.; Zdravkovic, V. Interaction ruling animal collective behavior depends on topological rather than metric distance: Evidence from a field study. *Proc. Natl. Acad. Sci. U.S.A.* **2008**, *105* (4), 1232−1237.
(161) Wang, W.; Duan, W.; Ahmed, S.; Sen, A.; Mallouk, T. E. From One to Many: Dynamic Assembly and Collective Behavior of Self-Propelled Colloidal Motors. *Acc. Chem. Res.* **2015**, *48* (7), 1938−1946.
(162) Ning, H.; Zhang, Y.; Zhu, H.; Ingham, A.; Huang, G.; Mei, Y.; Solovev, A. A. Geometry Design, Principles and Assembly of Micromotors. *Micromachines* **2018**, *9* (2), 75.
(163) Yan, J.; Bae, S. C.; Granick, S. Colloidal Superstructures Programmed into Magnetic Janus Particles. *Adv. Mater.* **2015**, *27* (5), 874−879.
(164) Zhang, J.; Alert, R.; Yan, J.; Wingreen, N. S.; Granick, S. Active phase separation by turning towards regions of higher density. *Nat. Phys.* **2021**, *17* (8), 961−967.
(165) Wu, C.; Dai, J.; Li, X.; Gao, L.; Wang, J.; Liu, J.; Zheng, J.; Zhan, X.; Chen, J.; Cheng, X.; Yang, M.; Tang, J. Ion-exchange enabled synthetic swarm. *Nat. Nanotechnol.* **2021**, *16* (3), 288−295.
(166) Lee, J. G.; Brooks, A. M.; Shelton, W. A.; Bishop, K. J. M.; Bharti, B. Directed propulsion of spherical particles along three dimensional helical trajectories. *Nat. Commun.* **2019**, *10*, 2575.
(167) Nishiguchi, D.; Iwasawa, J.; Jiang, H.-R.; Sano, M. Flagellar dynamics of chains of active Janus particles fueled by an AC electric field. *New J. Phys.* **2018**, *20*, 015002.
(168) Xie, H.; Sun, M.; Fan, X.; Lin, Z.; Chen, W.; Wang, L.; Dong, L.; He, Q. Reconfigurable magnetic microrobot swarm: Multimode transformation, locomotion, and manipulation. *Science Robotics* **2019**, *4* (28), eaav8006.
(169) Driscoll, M.; Delmotte, B.; Youssef, M.; Sacanna, S.; Donev, A.; Chaikin, P. Unstable fronts and motile structures formed by microrollers. *Nat. Phys.* **2017**, *13* (4), 375−379.
(170) Martinez-Pedrero, F.; Ortiz-Ambriz, A.; Pagonabarraga, I.; Tierno, P. Colloidal microworms propelling via a cooperative hydrodynamic conveyor belt. *Physical review letters* **2015**, *115* (13), 138301.
(171) Junot, G.; Cebers, A.; Tierno, P. Collective hydrodynamic transport of magnetic microrollers. *Soft Matter* **2021**, *17* (38), 8605−8611.
(172) Wang, W.; Giltinan, J.; Zakharchenko, S.; Sitti, M. Dynamic and programmable self-assembly of micro-rafts at the air-water interface. *Science Advances* **2017**, *3* (5), e1602522.
(173) Wang, W.; Gardi, G.; Malgaretti, P.; Kishore, V.; Koens, L.; Son, D.; Gilbert, H.; Wu, Z.; Harwani, P.; Lauga, E.; Holm, C.; Sitti, M. Order and information in the patterns of spinning magnetic micro-disks at the air-water interface. *Science Advances* **2022**, *8* (2), eabk0685.
(174) Gardi, G.; Ceron, S.; Wang, W.; Petersen, K.; Sitti, M. Microrobot collectives with reconfigurable morphologies, behaviors, and functions. *Nat. Commun.* **2022**, *13* (1), 2239.
(175) Huang, L.; Moran, J. L.; Wang, W. Designing chemical micromotors that communicate-A survey of experiments. *JCIS Open* **2021**, *2*, 100006.
(176) Wang, W.; Duan, W.; Ahmed, S.; Mallouk, T. E.; Sen, A. Small power: Autonomous nano- and micromotors propelled by self-generated gradients. *Nano Today* **2013**, *8* (5), 531−554.
(177) Brown, A.; Poon, W. Ionic effects in self-propelled Pt-coated Janus swimmers. *Soft Matter* **2014**, *10* (22), 4016−4027.
(178) Ebbens, S.; Gregory, D. A.; Dunderdale, G.; Howse, J. R.; Ibrahim, Y.; Liverpool, T. B.; Golestanian, R. Electrokinetic effects in catalytic platinum-insulator Janus swimmers. *Epl* **2014**, *106* (5), 58003.
(179) Brown, A. T.; Poon, W. C. K.; Holm, C.; de Graaf, J. Ionic screening and dissociation are crucial for understanding chemical self-propulsion in polar solvents. *Soft Matter* **2017**, *13* (6), 1200−1222.
(180) Hong, Y.; Diaz, M.; Cordova-Figueroa, U. M.; Sen, A. Light-Driven Titanium-Dioxide-Based Reversible Microfireworks and Micromotor/Micropump Systems. *Adv. Funct. Mater.* **2010**, *20* (10), 1568−1576.
(181) Sridhar, V.; Podjaski, F.; Kroeger, J.; Jimenez-Solano, A.; Park, B.-W.; Lotsch, B. V.; Siti, M. Carbon nitride-based light-driven microswimmers with intrinsic photocharging ability. *Proc. Natl. Acad. Sci. U.S.A.* **2020**, *117* (40), 24748−24756.
(182) Duan, S.; Xu, P.; Wang, W. Better fuels for photocatalytic micromotors: a case study of triethanolamine. *Chem. Commun.* **2021**, *57* (77), 9902−9905.
(183) Zhan, X.; Wang, J.; Xiong, Z.; Zhang, X.; Zhou, Y.; Zheng, J.; Chen, J.; Feng, S.-P.; Tang, J. Enhanced ion tolerance of electrokinetic locomotion in polyelectrolyte-coated microswimmer. *Nat. Commun.* **2019**, *10*, 3921.
(184) Peng, Y.; Xu, P.; Duan, S.; Liu, J.; Moran, J. L.; Wang, W. Generic Rules for Distinguishing Autophoretic Colloidal Motors. *Angew. Chem., Int. Ed.* **2022**, *61* (12), e202116041.
(185) Lu, Y.; Chen, S. C. Micro and nano-fabrication of biodegradable polymers for drug delivery. *Adv. Drug Delivery Rev.* **2004**, *56* (11), 1621−1633.
(186) Hortelao, A. C.; Simó, C.; Guix, M.; Guallar-Garrido, S.; Julián, E.; Vilela, D.; Rejc, L.; Ramos-Cabrer, P.; Cossío, U.; Gómez-Vallejo, V. Swarming behavior and in vivo monitoring of enzymatic nanomotors within the bladder. *Science Robotics* **2021**, *6* (52), eabd2823.
(187) Yang, L.; Zhang, L. Motion Control in Magnetic Microrobotics: From Individual and Multiple Robots to Swarms. *Annual Review of Control, Robotics, and Autonomous Systems* **2021**, *4*, 509−534.
(188) Wang, Q.; Yang, L.; Yu, J.; Chiu, P. W. Y.; Zheng, Y.-P.; Zhang, L. Real-Time Magnetic Navigation of a Rotating Colloidal Microswarm Under Ultrasound Guidance. *Ieee Transactions on Biomedical Engineering* **2020**, *67* (12), 3403−3412.

(189) Peskin, C. S.; Odell, G. M.; Oster, G. F. Cellular motions and thermal fluctuations: the Brownian ratchet. *Biophys. J.* **1993**, *65* (1), 316−324.
(190) Turiv, T.; Koizumi, R.; Thijssen, K.; Genkin, M. M.; Yu, H.; Peng, C.; Wei, Q.-H.; Yeomans, J. M.; Aranson, I. S.; Doostmohammadi, A.; Lavrentovich, O. D. Polar jets of swimming bacteria condensed by a patterned liquid crystal. *Nat. Phys.* **2020**, *16* (4), 481−487.
(191) Genkin, M. M.; Sokolov, A.; Lavrentovich, O. D.; Aranson, I. S. Topological Defects in a Living Nematic Ensnare Swimming Bacteria. *Physical Review X* **2017**, *7* (1), 011029.
(192) Wei, F.; Yin, C.; Zheng, J.; Zhan, Z.; Yao, L. Rise of cyborg microrobot: different story for different configuration. *Iet Nanobiotechnology* **2019**, *13* (7), 651−664.
(193) Alapan, Y.; Yasa, O.; Yigit, B.; Yasa, I. C.; Erkoc, P.; Sitti, M. *Microrobotics and Microorganisms: Biohybrid Autonomous Cellular Robots* **2019**, *2*, 205−230.
(194) Sun, L.; Yu, Y.; Chen, Z.; Bian, F.; Ye, F.; Sun, L.; Zhao, Y. Biohybrid robotics with living cell actuation. *Chem. Soc. Rev.* **2020**, *49* (12), 4043−4069.
(195) Petroff, A. P.; Wu, X.-L.; Libchaber, A. Fast-Moving Bacteria Self-Organize into Active Two-Dimensional Crystals of Rotating Cells. *Phys. Rev. Lett.* **2015**, *114* (15), 158102.
(196) Huang, M.; Hu, W.; Yang, S.; Liu, Q.-X.; Zhang, H. P. Circular swimming motility and disordered hyperuniform state in an algae system. *Proc. Natl. Acad. Sci. U.S.A.* **2021**, *118* (18), e2100493118.
(197) Tan, T. H.; Mietke, A.; Li, J.; Chen, Y.; Higinbotham, H.; Foster, P. J.; Gokhale, S.; Dunkel, J.; Fakhri, N. Odd dynamics of living chiral crystals. *Nature* **2022**, *607* (7918), 287−293.

https://doi.org/10.1021/acsnano.2c11680
ACS Nano 2023, 17, 11969−11993